Structural Optimization with Fatigue Constraints

Oest, Jacob

Publication date:
2017

Document Version
Publisher's PDF, also known as Version of record

Link to publication from Aalborg University

Citation for published version (APA):
Oest, J. (2017). *Structural Optimization with Fatigue Constraints*. Aalborg Universitetsforlag.

STRUCTURAL OPTIMIZATION WITH FATIGUE CONSTRAINTS

BY
JACOB OEST

DISSERTATION SUBMITTED 2017

AALBORG UNIVERSITY
DENMARK

Structural Optimization with Fatigue Constraints

Jacob Oest

Department of Materials and Production
Solid and Computational Mechanics Group
Aalborg University, Denmark

PhD Thesis
2017

Dissertation submitted: August, 2017

PhD supervisor: Professor, PhD, MSc Erik Lund
Aalborg University

Assistant PhD supervisor: Associate Professor, PhD, MSc Lars C. T. Overgaard
Aalborg University

PhD committee: Associate Professor Jens H. Andreasen (chairman)
Aalborg University, Denmark

Technology Director Claus B.W. Pedersen
Dassult Systemes Deutschland GmbH, Germany

Professor Helder C. Rodrigues
Instituto Superior Técnico, Portugal

PhD Series: Faculty of Engineering and Science, Aalborg University

Department: Department of Materials and Production

ISSN (online): 2446-1636
ISBN (online): 978-87-7210-034-0

Published by:
Aalborg University Press
Skjernvej 4A, 2nd floor
DK – 9220 Aalborg Ø
Phone: +45 99407140
aauf@forlag.aau.dk
forlag.aau.dk

Printed in Denmark by Rosendahls, 2017

Preface

This thesis has been submitted to the Faculty of Engineering and Science at Aalborg University in partial fulfillment of the requirements for the degree of Doctor of Philosophy in Mechanical Engineering. The work has been carried out at the Department of Materials and Production at Aalborg University in the period from August 2014 to July 2017. The work is part of the research project entitled *ABYSS - Advancing BeYond Shallow waterS - Optimal design of offshore wind turbine support structures* which has been funded by the Danish Council for Strategic Research, grant no. 13005-00020B. This support is gratefully acknowledged.

I would like to express my sincere gratitude to my main supervisor Professor Erik Lund for the most competent guidance. Thank you for all our talks and discussions which always inspired and motivated me, and thank you for your joyful spirit which made everyday work and conference attendances even better. I would also like to thank my co-supervisor Associate Professor Lars Christian Terndrup Overgaard for providing insightful knowledge and experience from the wind energy industry during the first part of my PhD study. I am also thankful for the collaboration with René Sørensen, where I especially enjoyed our many talks on optimization algorithms and physical behavior of the problem at hand. My thanks also goes to Professor Michael Muskulus and project leader Professor Mathias Stolpe for receiving and guiding me during my two brief research stays at NTNU and DTU, respectively.

A special thanks to my fellow PhD candidates and co-authors Kasper Sandal, Sebastian Schafhirt, and Lars Einar S. Stieng for your competent work and dedication, and for showing me a good time in Trondheim. Lastly, I would like to extend my gratitude to all my co-workers at the Solid and Computational Mechanics group for providing a great working environment. It has been a true pleasure.

Aalborg, August 2017

Jacob Oest

Abstract

Fatigue is one of the most important causes of mechanical failure. Fatigue can be described as progressive damage to a material subject to repeated loading. Most fatigue-loaded components are exposed to a large amount of repeated loads where the stresses are low and the strains are elastic. This is normally referred to as high-cycle fatigue. This dissemination addresses structural optimization for high-cycle fatigue in metals.

The developed methods take offset in the offshore wind industry, more specifically in the design of a lattice-type of support structure for large wind turbines. These so-called jacket structures are subjected to complex aerodynamic and hydrodynamic loading conditions throughout their lifespan of approximately 20-25 years. The design of these structures is generally driven by fatigue in welded connections, and constitutes a great application for fatigue optimization. Thus, a new approach to optimization of jacket structures has been established. Additionally, this method and other state-of-the-art approaches to gradient-based optimizations of jacket structures are investigated and compared. The sizing optimization of jacket structures is of large interest to the industry, and is an optimization problem with few design variables, many constraints, and very computational costly analyses due to the large multiaxial and non-proportional load cases.

Topology optimization of 2D continua with fatigue constraints is also addressed. This problem differs from structural optimization of jackets, as many design variables are present in topology optimization. An effective formulation is proposed for proportional loading conditions, where finite-life constraints are formulated such that the computational costs of the design sensitivity analysis is comparable to static stress optimization.

Resumé

Udmattelsesbrud, også kaldet materialetræthed, er en af de mest vigtige årsager til mekanisk svigt. Udmattelse kan beskrives som progressiv skade i et materiale under varierende belastning. De fleste komponenter i risiko for udmattelsesbrud er udsat for mange varierende laster, hvor spændingerne er lave og tøjningerne elastiske. Denne afhandling omhandler strukturel optimering for udmattelsesbrud af komponenter udsat for et stort antal cykliske laster.

De udviklede metoder er udarbejdet med henblik på offshore vindmølleindustrien, mere specifikt på design af gitter-substrukturer til store vindmøller. En sådan type struktur er den såkaldte jacket. Jacket-strukturer er udsat for komplekse aerodynamiske og hydrodynamiske laster i løbet af strukturens levetid, der typisk er 20-25 år. Udmattelsesbrud i svejsninger er et designdrivende kriterie for jacket-strukturen, hvorfor design af denne struktur er oplagt at udføre med optimeringsmetoder mod udmattelse. Derfor er en ny metode til strukturel optimering af jacket-strukturer blevet udviklet. Denne metode er endvidere blevet undersøgt og sammenlignet med andre state-of-the-art metoder til optimering af jackets. Tværsnitsoptimering af jacket-strukturer er af stor interesse for industrien. Det udgør et optimeringsproblem med få designvariable, mange bibetingelser, og en beregningstung analyse grundet de store multiaksiale og ikke-proportionale lastserier.

En metode til topologioptimering i 2D med udmattelse som bibetingelse er også udviklet. Dette optimeringsproblem adskiller sig fra optimeringen af en jacket, primært da der er mange designvariable i topologioptimering. Der er blevet udviklet en effektiv formulering af topologioptimering til en given levetid under proportionale lastserier. Beregningstiden i den nye metode er sammenlignelig med spændingsoptimering for en statisk last.

Thesis Details

This dissertation serves as an introduction to the research areas of the PhD project. The dissertation is made as a collection of scientific papers for publication in refereed journals. Two journal papers are published in refereed scientific journals and one journal paper is submitted.

Thesis Title:	Structural Optimization with Fatigue Constraints
PhD Student:	Jacob Oest
PhD Supervisors:	Erik Lund Professor, PhD, MSc Department of Materials and Production Aalborg University, Denmark
	Lars Christian Terndrup Overgaard Associate Professor, PhD, MSc Department of Materials and Production Aalborg University, Denmark

Publications in refereed journals

A) J Oest, R Sørensen, LCT Overgaard, and E Lund. Structural optimization with fatigue and ultimate limit constraints of jacket structures for large offshore wind turbines. *Structural and Multidisciplinary Optimization*, 55(3):779-793, 2017.

B) J Oest, K Sandal, S Schafhirt, LES Stieng, and M Muskulus. On gradient-based optimization of jacket structures for offshore wind turbines. *under review*, pages 1-15, 2017.

C) J Oest and E Lund. Topology optimization with finite-life fatigue constraints. *Structural and Multidisciplinary Optimization*, pages 1-15, 2017. DOI: 10.1007/s00158-017-1701-9

Publications in proceedings with review

D) J Oest, LCT Overgaard, and E Lund. Gradient based structural optimization with fatigue constraints of jacket structures for offshore wind turbines. *Proceedings of*

11th World Congress on Structural and Multidisciplinary Optimization, Sydney, Australia, June 7-12, pages 1-6, 2015.

E) J Oest, R Sørensen, LCT Overgaard, and E Lund. Gradient based structural optimization of jacket structures with fatigue and ultimate limit state constraints for offshore wind turbines. *Proceedings of ECCOMAS Congress 2016*, Hersonissos, Greece, June 5-10, pages 1, 2016.

F) J Oest and E Lund. Finite-life fatigue topology optimization using a density approach. *Book of Abstracts of 12th World Congress on Structural and Multidisciplinary Optimization*, Braunschweig, Germany, June 5-9, pages 1, 2017.

G) J Oest, K Sandal, S Schafhirt, LES Stieng, and M Muskulus. Comparison of fatigue constraints in optimal design of jacket structures for offshore wind turbines", *Book of Abstracts of 12th World Congress on Structural and Multidisciplinary Optimization*. Braunschweig, Germany, June 5-9, pages 1, 2017.

H) J Oest and E Lund. On 2D topology optimization of fatigue constrained problems. *Book of Abstracts to 22nd International Conference on Computer Methods in Mechanics*, Lublin, Poland, September 13-16, accepted, pages 1-2, 2017.

This thesis has been submitted for assessment in partial fulfillment of the PhD degree. The thesis is based on the submitted or published scientific papers which are listed above. Parts of the papers are used directly or indirectly in the extended summary of the thesis. As part of the assessment, co-author statements have been made available to the assessment committee and are also available at the Faculty. The thesis is not in its present form acceptable for open publication but only in limited and closed circulation as copyright may not be ensured.

Contents

Preface iii

Abstract v

Resumé vii

Thesis Details ix

1 Introduction 1
1.1 Introduction to the PhD study 1
1.2 Wind energy 1
1.3 Wind turbines and support structures 2
1.4 Fatigue failure 5
1.5 Optimization methods 6
1.6 Objectives of the PhD project 8

2 State-of-the-art 9
2.1 Structural optimization of support structures 9
2.1.1 Finite element analysis of jacket support structures 12
2.1.2 Loading conditions 13
2.1.3 Fatigue limit state analysis 19
2.1.4 Ultimate limit state analysis 22
2.1.5 Frequency analysis 23
2.1.6 Design sensitivity analysis 23
2.2 Topology optimization with fatigue constraints 26
2.2.1 Topology optimization 26
2.2.2 Stress-based topology optimization 28
2.2.3 Fatigue-based topology optimization 32

3 Summary of Results and Conclusion 37
3.1 Description of Papers 37
3.1.1 Paper A 37
3.1.2 Paper B 38
3.1.3 Paper C 39
3.2 Conclusions and contributions 40

3.3 Future work 41

References **43**

A Structural optimization with fatigue and ultimate limit constraints of jacket structures for large offshore wind turbines **53**

B On gradient-based optimization of jacket structures for offshore wind turbines **55**

C Topology optimization with finite-life fatigue constraints **57**

Chapter 1

Introduction

This chapter provides a brief introduction to the overall research project and the research undertaken in this PhD study.

1.1 Introduction to the PhD study

This PhD study is part of a larger research project *ABYSS - Advancing BeYond Shallow waterS - Optimal design of offshore wind turbine support structures* sponsored by the Danish Council for Strategic Research. The aim of the project is to develop a numerical optimization tool to aid in the design of support structures for large offshore wind turbines. The tool will utilize gradient-based optimization techniques to design mass-producible and reliable support structures for deep waters and large turbines. This will in turn provide a decrease in levelized cost of energy which will aid in achieving sustainable energy goals. While this tool is very specific in nature, the developed methods are immediately applicable to other industrial designs, e.g. aerospace structures. A total of eight partners ensure expertise within research, offshore wind energy, foundation design, and design system development. Besides Aalborg University, the partners involved in the project are DTU Wind Energy, DTU Civil Engineering, NTNU Civil and Environmental Engineering, Dassault Systémes, SINTEF Energy Research, DONG Energy A/S, and Universal Foundation A/S. This PhD study addresses the fatigue optimization part of the project. Thus, the main topic of this thesis is methods for effective gradient-based structural optimization with fatigue constraints.

1.2 Wind energy

Greenhouse gas emission is well known to be the primary cause of global warming. Consequently, most countries are committed to international and national renewable energy goals. Thus, the demand for reliable and sustainable energy is ever growing. Wind energy is among the most popular renewable energy sources, which can be partly explained by the low levelized cost of electricity. While wind energy has a high initial cost, the costs are generally less sensitive to changes than more conventional energy sources such as fossil fuels. Additionally, wind power is an immense source of energy with a theoretical potential estimated to 253 TW, which is sufficient to cover the current world energy consumption several times (Jacobson and Archer, 2012).

Onshore wind energy is a mature industry where the levelized cost of energy can compete with conventional energy sources. Installation is relatively easy, and inspection and maintenance costs are low. In 2014, the International Renewable Energy Agency estimated the cost of onshore projects to 0.06-0.12 USD/kWh and offshore projects to 0.10-0.21 USD/kWh (International Renewable Energy Agency, 2015). Due to the low costs associated with onshore energy, 420 GW out of a total of 432 GW installed by the end of 2015 is installed onshore (Konstantinidis and Botsaris, 2016). However, onshore sites are often very limited. Additionally, visual impact, noise pollution, impact on tourism, reduction in land value, and ecosystem-related issues affecting flora and fauna are large drawbacks of onshore wind farms.

Offshore wind energy has an increased initial cost and a relatively high cost of operation and maintenance as compared with onshore wind energy. However, due to stronger winds and large continuous available installation sites, offshore wind energy is a rapidly growing industry with many countries committing to large offshore wind farms. For instance, China has a target of installing 30 GW off offshore wind energy by 2020 (The Carbon Trust, 2014). The large increase in demand of offshore wind energy is strongly coupled to a decreasing levelized cost of energy. The company Vattenfall won the tender to build the Danish 600 MW offshore site Kriegers Flak with a record price of just 49.9 EUR/MWh, which is approximately 0.06 USD/kWh. Lastly, as compared with onshore wind farms, visual impact and noise are less of a concern for offshore wind parks.

1.3 Wind turbines and support structures

A large Horizontal Axis Wind Turbine (HAWT) can be described by a few overall main components. From the top, a typically three-bladed rotor is converting part of the kinetic energy of the wind through lift into mechanical energy that rotates a main shaft. The rotating shaft enters a generator that converts the mechanical energy to electrical energy. The generator is located inside the nacelle, a large box-like housing cover, that contains most of the mechanical and electrical equipment in a wind turbine. On upwind turbines, there is a yawing system just below the nacelle to ensure that the turbine is facing towards the wind direction. When modeling a wind turbine, engineers often refer to these components collectively as the Rotor-Nacelle Assembly (RNA). Roughly speaking, everything below the RNA can be considered the support structure.

Many variations of support structures exist. On concept level there are either bottom fixed support structures or the emerging floating support structures. Some of the types of support structures are shown in Fig. 1.1. Common for every type of support is that they are attached to the RNA by a tower. The tower consists, in most cases, of slightly conical tubular steel members that are typically manufactured in sections of 20-30 m. For onshore turbines, the tower spans all the way to the ground where it is fixed to the turbine foundation. Different turbine foundation types exist where the geotechnical conditions of the soil at the installation site together with the turbine size and type governs the choice of foundation. For offshore wind turbines, the tower is connected to a substructure by a Transition Piece (TP).

The type of substructure and TP depends on preference and installation site. Most offshore wind turbines have been installed in shallow waters. At such sites, the monopile substructure, see Fig. 1.1 (a), is the typical choice. The monopile is relatively easy to install and has low production costs. Moreover, the monopile is a proven technology, which is very important for funding (Seidel, 2014). For a monopile, the TP typically consists of a conical connection, where small brackets on the inside of the bottom of the tower temporarily carry the load before a grouted connection between tower and monopile can be established. Some issues with this type of grouted connection have occurred, and it is estimated to be an industry-wide problem affecting hundreds of towers. For instance in Horns Rev I, settlements of the foundation have been found. Thus, the brackets carry part of the in-service loading. However, they are only designed to carry a temporary load during installation. Monopiles are in general feasible to about 30 m of water depth. In deeper waters the fabrication costs can be too high and installation processes such as pile driving may become too problematic (de Vries, 2011). It must be noted that a new generation of monopiles, the so-called XL monopiles, are being developed with the aim of installation in deeper waters.

Since shallow water sites are limited, the industry is also providing solutions for deeper waters. For a water depth of approximately 30-60 m the three or four-legged jacket, see Fig. 1.1 (d-e), is currently considered the most cost effective solution. Floating support structures are also applicable in this water depth. Floating support structures have a large advantage in installation costs. However, the concept of floating support structures is still in a very preliminary stage, with the first floating offshore wind park Hywind Scotland Pilot Park with five 6 MW turbines beginning production in 2017. Many of the floating support solutions are feasible for a large range of water depths, including very deep waters. The Hywind Scotland Pilot Park is going to be installed in approximately 95-120 m deep water.

Jacket structures have been used in the oil and gas industry for many years, therefore much knowhow and many production facilities already exist. While this gives invaluable insight into the structure and design process, both the supply chain and structural demands are very different in the wind energy sector as compared with the oil and gas sector. Therefore, the costs of jackets are projected to decrease significantly when better mass-production facilities that are specialized to provide jackets for wind energy purposes are established.

Jacket structures are much less sensitive to hydrodynamic loading as compared with monopiles, and they are both light and stable structures. Additionally, the environmental impact of the installation process is much less, as the piles driven into the seabed are much smaller in diameter. It is projected that for installation site types that are 125 km from port and are 35 m deep and use 8 MW turbines, jackets will be used for almost half of the market in 2020, and three quarters of the market in 2025 (Valpy and English, 2014). In sites of 35 m of water depth jackets are attractive since they typically require 40-50% less steel as compared with monopiles (Qyatt et al., 2014). However, the jacket is more complex to produce due to the large number of welded connections, and is also more difficult to install due to the complex piling pro-

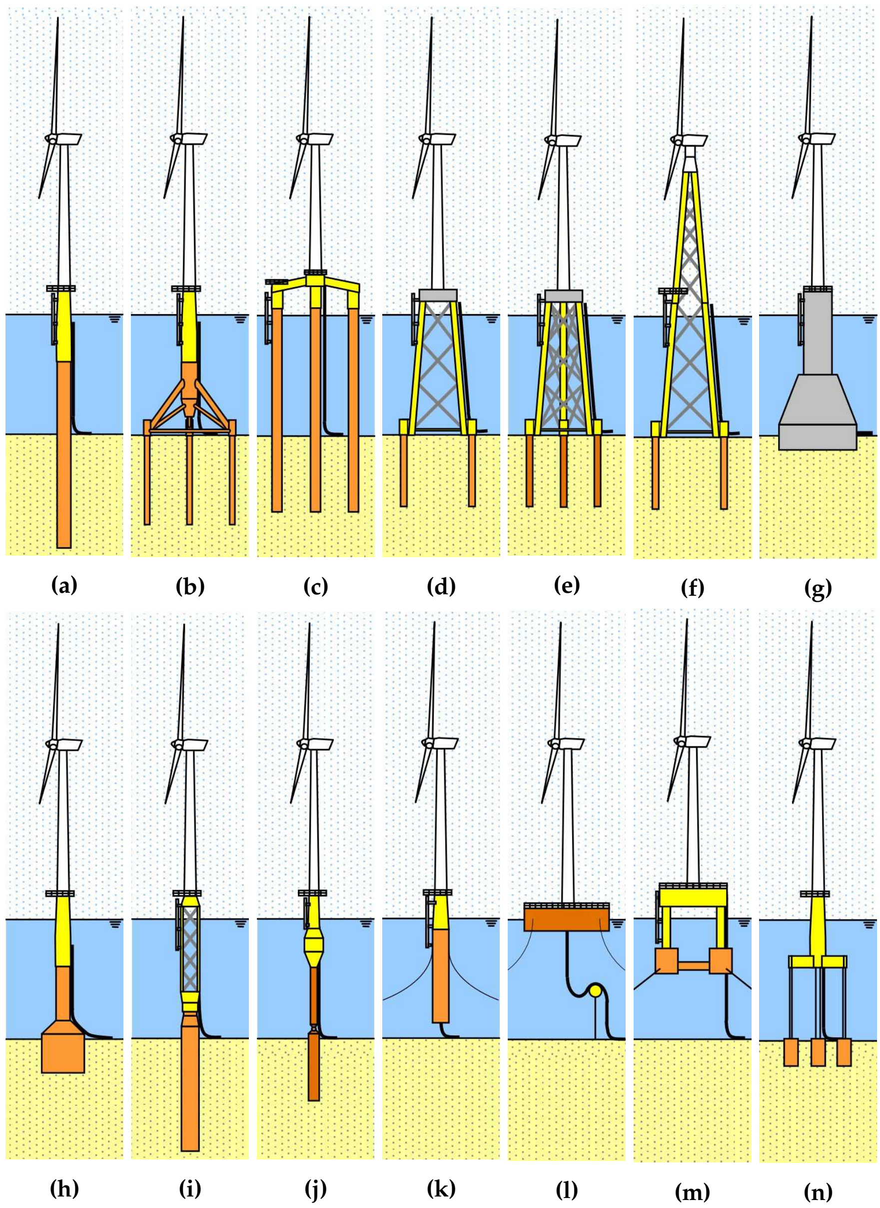

Fig. 1.1: Different types of support structures for offshore wind turbines. **(a)** Monopile, **(b)** tripod, **(c)** tripile, **(d)** jacket, **(e)** three-legged jacket, **(f)** full-height lattice tower, **(g)** gravity base structure, **(h)** suction bucket monotower, **(i)** full truss tower, **(j)** compliant structure, **(k)** spar floater, **(l)** barge floater, **(m)** semi-submersible floater, **(n)** tension leg. Figures adapted from de Vries (2011).

(a) (b)

Fig. 1.2: **(a)** OWEC jacket being transported to Alpha Ventus, Germany. **(b)** Senvion 5 MW turbines installed at Alpha Ventus. Courtesy of offshorewind.biz and power-technology.com.

cess that requires high precision. Thus, it is important to develop new and effective design methods for jacket structures for wind turbines to ensure that the levelized cost of offshore wind energy on deeper waters is comparable to shallow waters. One of the important failure modes to consider when designing jacket structures is fatigue.

1.4 Fatigue failure

Fatigue is progressive weakening of a material subjected to cyclic loading conditions. The fatigue process involves both crack initiation, crack propagation, and structural failure.

Fatigue is one of the most important failure modes in engineering, being responsible for approximately 50% to 90% of all mechanical failures (Stephens et al., 2000). In 1978 it was estimated that fracture-related costs in the United States were 99 billion USD (in 1978 dollars), corresponding to 4.4% of the gross national product (Reed et al., 1983). Fatigue is a local phenomena, that is generally caused by an excess of deformations. Thus, it is imperative to understand the stress and strain state of a fatigue-loaded structure in order to adequately investigate for fatigue. Overall, two types of fatigue exist, i.e. low-cycle fatigue and high-cycle fatigue.

Low-cycle metal fatigue is typically associated with plastic deformations, and the low-cycle fatigue analysis is often based on strain-based models. Due to the plastic deformations, low-cycle fatigue models often include work hardening/softening. Generally speaking, low-cycle fatigue is when fatigue failure occurs with less than $10,000$ load cycles. High-cycle metal fatigue is often investigated using stress-based models as the material typically only experiences elastic deformations.

An excessive amount of different fatigue criteria exist for both low- and high-cycle fatigue of metals. The criteria depend on the material properties (ductile or brittle material), loading conditions (proportional or non-proportional, uniaxial or multiaxial), and depending on the specimen investigated (surface treatments, notch effects, ambient temperature) etc.

Fatigue in metals is still an ongoing research subject, where especially multiaxial and non-proportional loading is investigated (Socie and Marquis, 1999). This type of loading condition is very common in engineering, e.g. in a jacket structure for an offshore wind turbine. In this work it is investigated how gradient-based techniques for structural optimization including fatigue can be formulated.

1.5 Optimization methods

Engineering optimization, sometimes referred to as design optimization, is a method of applying mathematical optimization techniques to engineering problems. Mathematical optimization can be described as finding optimal values for a set of parameters (design variables), that minimize or maximize a cost function (the objective function), while satisfying the problem constraints. Applied to mechanical engineering, this could be finding an optimal shape of a side mirror in a car, that minimizes the drag while still satisfying manufacturing constraints, design constraints, and structural integrity constraints. This example can naturally also be handled by conventional design methods based on intuition, experience, and heuristics. However, conventional design methods often have a very strict limit on the allowable design iterations before it becomes too costly to further optimize a design. Using a mathematical optimization approach, numerous design iterations can be achieved in very little time.

Structural optimization is typically addressed using at least one of the following three optimization methods: (i) sizing optimization, (ii) shape optimization, and/or (iii) topology optimization, see Fig. 1.3. Sizing optimization is finding an optimized size of a design by varying sizing parameters such as thickness, diameter, length, and width. This method often requires some conceptual design before being applicable, e.g. an initial jacket design based on a 8 MW turbine, which needs to be adapted to withstand the loads from a 10 MW turbine. This can be achieved by optimizing the cross sectional properties of the jacket. Shape optimization is defining the outer geometry of a given structure. Again, some initial design needs to be provided. Topology optimization can be thought of as an optimal material distribution problem within a specified design domain. This method has a very large design freedom, and often very little needs to be known about the optimal material distribution beforehand. In this thesis, both sizing and topology optimization are addressed.

The optimization problem must be solved using an adequate technique. Many different optimization techniques exist to solve nonlinear programming problems, but they can generally be classified by three methods. The three methods are zero-order methods like metaheuristics, first-order methods such as Sequential Linear Programming (SLP), and second order methods like Sequential Quadratic Programming (SQP).

Zero-order methods such as metaheuristics only rely on cost and constraint function values. Therefore, zero-order methods are also referred to as gradient-free methods. The methods are very easy to apply to even very complicated structural analysis

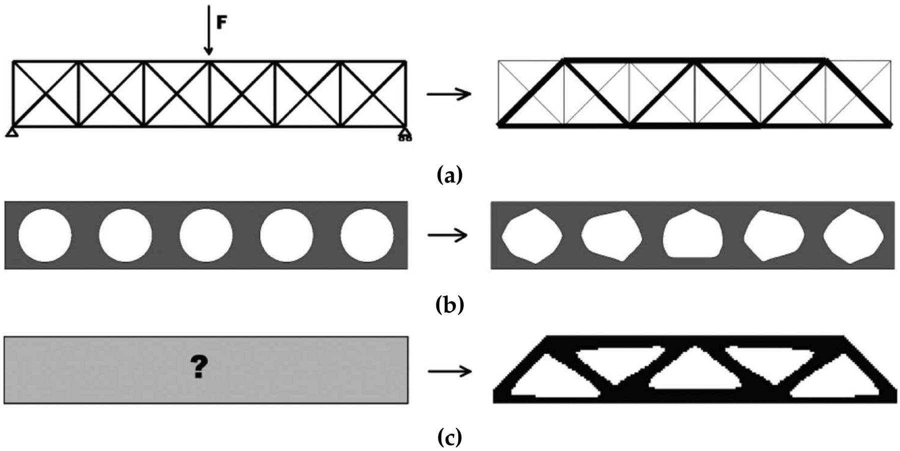

Fig. 1.3: **(a)**: Sizing optimization, **(b)**: Shape optimization, **(c)**: Topology optimization. Figure adapted from Bendsøe and Sigmund (2004).

problems. Most metaheuristics are based on observations in nature where some of the more popular algorithms are Genetic algorithm (GA, see Deb et al. (2002)), Particle Swarm Optimization (PSO, see Kennedy (2011)), and Simulated Annealing (SA, see Kirkpatrick et al. (1983)). A large amount of metaheuristics exists, but common for all is that they, in general, need many more function evaluations than SLP and SQP methods before reaching an optimum. Metaheuristics are used widely in both research and in industry, and the large appeal of the methods lie in the fast and easy implementation of the methods.

First-order methods like SLP is a class of methods that utilize the gradients (Jacobian) of the cost and constraint functions with respect to the design variables to solve first order approximations of the model. Thus, a Design Sensitivity Analysis (DSA) must be performed, which for implicit structural problems can be very computationally expensive. It is a requirement that the optimization problem is at least once differentiable. If the sensitivity analysis can be performed effectively, it can be a much faster approach than e.g. metaheuristics, since much fewer function evaluations are typically necessary.

Second-order methods like SQP require second-order information (Hessian) of the objective and constraint functions. The second-order derivatives can be computationally expensive and difficult to evaluate and is therefore often approximated using first-order information. SQP methods generally converge faster than both metaheuristics and SLP approaches, as more information is provided to the optimization algorithm.

There exists a variety of other first- and second-order optimization algorithms for structural optimization, but they have not been applied in the innovations of this PhD study and is therefore outside the scope of this thesis.

1.6 Objectives of the PhD project

The overall objective of the PhD study is to develop analytical gradient-based optimization methods for fatigue-loaded structures applicable to the design of offshore wind turbine substructures. The methods are developed within a finite element framework such that the methods are generic, and such that they can be combined with work from other partners within the ABYSS project. The methods must be viable for both conceptual and preliminary design of offshore wind turbines. The primary topics are:

- Effective finite-life fatigue sizing optimization of jacket structures considering large load cases and offshore standards.
- Validity of different gradient-based optimization approaches to optimal design of jacket structures.
- Identification of important structural parameters from an optimization point-of-view.
- Topology optimization for fatigue.

These topics have been decided partly by the original research application, partly by discussions with partners in the project, and partly by the authors personal desire to investigate certain aspects of fatigue-constrained structural optimization.

Chapter 2

State-of-the-art

This section is comprised of two parts. One part describes state-of-the-art of optimization of support structures for offshore wind turbines, while the second part describes state-of-the art topology optimization with fatigue constraints. The section will also give a brief introduction to the key methodologies applied by the author.

2.1 Structural optimization of support structures

The optimal design of support structures for wind turbines is a nontrivial task (Muskulus and Schafhirt, 2014). A wind turbine consists of numerous structural and electrical parts that are highly coupled. Thus, in an ideal optimization framework, all components should be treated as design variables and analyzed in time-domain considering all effects and non-linearities. Additionally, the optimization should be fully coupled to a wind farm layout optimization including site- and weather data and wake effects. This is currently not near possible. Therefore, it is common practice to optimize for a specific part of the wind turbine individually well-knowing that it affects the performance of other parts. This section seeks to first describe the difficulties involved in modeling and optimization of offshore support structures for wind turbines, and secondly to present an overview of state-of-the-art research in the field of structural optimization of support structures.

Wind turbine support structures must typically withstand highly complex loading conditions for 20 years. The larger turbines used today have very flexible blades that are very susceptible to dynamic effects. Both the aerodynamic and hydrodynamic loadings are difficult to determine and are both exposed to environmental changes. The wind flow is turbulent, and in most wind farms, direction-dependent wake effects are present. Wave loads and currents are also affecting the structure, and can have a large influence on the structural design. Certain special environmental phenomena may occur and must also be addressed, e.g. wind gusts and 50-year waves.

Soil-conditions can vary and are typically time-dependent due to soil stiffening effects. Additionally, jackets are submerged in seawater with varying salinity and temperature. The jackets are also exposed to microbiological influenced corrosion.

Corrosion can typically be detected and addressed by divers. However, this is an expensive process, and corrosion on the inside of flooded members cannot be investigated by divers.

The numerical simulations of offshore wind turbines are very computationally expensive. In state-of-the-art simulation software, the rotor models are typically based on Blade Element Momentum theory (BEM), and the software are capable of predicting large deflections, and handle complex dynamic inflow and dynamic stall. Different wind, turbulence, and wake models are also available in most software. The structural parts are typically modeled using multibody formulations with linear Timoshenko or Bernoulli-Euler beam elements. Most software computes hydrodynamic loading using Morrison equation, based on different types of water kinematic models. Typically, linear wave theory is applied.

Numerical optimization methods can assist in the design of support structures to find near optimal designs. However, due to the complexity and large amount of load cases, state-of-the-art optimization methods are primarily being applied in the preliminary design phase. In this phase, many assumptions can be made to reduce both the simulation complexity and the computational cost.

Gradient-free methods have been applied in the optimization of support structures. The primary arguments of choosing gradient-free methods in this framework is that the analyses are highly complex and some part of the analysis code may be non-differentiable. Additionally, it is easy to implement discrete variables in the optimization, which is typically difficult with gradient-based optimization. The downside to gradient-free methods, in this setting, is that the simulations are typically very time-consuming, and it is therefore desirable to have as few function evaluations as possible.

To greatly reduce the computational costs, static loads are widely applied in the optimal design of support structures problem. In Uys et al. (2007) an onshore monopile structure is optimized with respect to manufacturing and material costs by varying the ring stiffeners using a search algorithm. The optimization is constrained by buckling constraints and static wind loads are applied. Long et al. (2011) present an improved design of a full-height lattice tower by altering the bottom leg distance (the footprint) while satisfying buckling constraints. In Perelmuter and Yurchenko (2013), a monopile tower height and diameters and thicknesses are optimized subject to Ultimate Limit State (ULS) constraints. Dynamic factors are included to account for fluctuations in the wind loads. In Gentils et al. (2017), an offshore monopile is optimized by combining commercial analysis software with a genetic algorithm. In their optimization, they consider both Fatigue Limit State (FLS) and ULS constraints. The fatigue load is reduced to a static load using the Damage Equivalent Load (DEL) method, as explained in Section 2.1.3.

Frequency domain analysis is often applied in wind energy engineering due to the computational benefits. In the frequency domain, many load series can be investigated in a very short time. Optimization of support structures using frequency analysis is investigated in Thiry et al. (2011). They optimize a monopile structure using a genetic algorithm and consider both ULS and FLS constraints, but disregard aerodynamic damping and assume a rigid rotor. In Long and Moe (2012), the bottom leg distance of a tripod is improved based on a frequency domain analysis and fatigue constraints. The aerodynamic damping is estimated using a linear dashpot element. They compare their design for FLS with their design for ULS and find that the fatigue-driven design is heavier.

Time-domain analysis is the approach recommended by offshore standards. However, it is also by far the most computationally expensive approach. Some of the first work on optimization of support structures modeled in time-domain is demonstrated in Yoshida (2006), where an integrated analysis is combined with a genetic algorithm to optimize an onshore monopile. The diameters, wall thicknesses, and the locations of flanges on the tower are optimized. Using state-of-the-art integrated analysis software the modeling accuracy is high, but so are the computational costs. In Zwick et al. (2012) a full-height lattice tower is optimized for member thickness. One load time-history is included and recalculated in each design iteration. It is observed that there exists a weak coupling between members. In Schafhirt et al. (2016) the weak coupling is exploited, and the Stress Concentration Factors of connections (SCFs, explained in detail in Section 2.1.2) are optimized independently of the structural analysis. In Pasamontes et al. (2014) and in Schafhirt et al. (2014), a genetic algorithm is applied to the optimization of a jacket structure subject to FLS and ULS constraints. The analysis is performed using integrated software, and only one load case is included in both works.

Gradient-based optimization with finite difference approximated gradients have also been applied to support structures analyzed in time-domain. Finite-difference schemes can be effective as only function evaluations are necessary. Thus, the implementation work is near equivalent of gradient-free methods. However, it has been observed that finite difference approximations of especially FLS constraints are highly perturbation dependent (Chew et al., 2015; Oest et al., 2017b; Chew, 2017). In Ashuri et al. (2014) reduction of the levelized cost of energy is achieved by gradient-based optimization of turbine and tower. The gradients are determined by finite difference schemes. ULS, FLS and frequency constraints are included. The work was extended to include wind farm layout optimization in Ashuri et al. (2016). The industrial demonstration of a jacket optimization in Gerzen et al. (2017) uses a semi-analytical adjoint formulation of the design sensitivities of the fatigue constraints. In their work, the welded sections are modeled using shell elements, and they optimize for thickness. The many weld nodes are aggregated using P-norm functions into 48 constraints corresponding to one constraint in each weld line.

Recently, analytical gradient-based optimization of support structures has been developed. In Chew et al. (2016); Chew (2017) optimization of a jacket structure considering frequency, ULS and FLS constraints is solved. The aerodynamic loading is based on a bottom-fixed turbine, and the aerodynamic damping is estimated by a spring and a dash-pot at tower top in the fore-aft direction. The optimization includes a large amount of loads in the fatigue analysis and they consider all relevant wind-speeds.

It must be mentioned that other approaches to structural optimization of offshore structures exist, e.g. probabilistic and robust optimizations, but they are not covered in this thesis.

The following section gives a brief introduction to a state-of-the-art approach to gradient-based optimization of jacket structures. The framework is limited to opti-

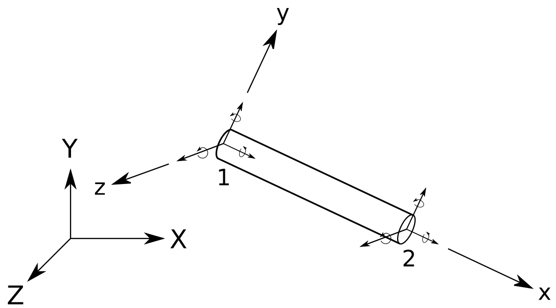

Fig. 2.1: Beam element with local coordinates (x,y,z) and global coordinates (X,Y,Z).

mization of diameters and wall-thicknesses in time-domain using beam finite element theory. Both static (DEL), quasi-static, and dynamic modeling is applied. Methods of generating aerodynamic and hydrodynamic loads are presented. The fatigue analysis and design sensitivities using each of the three methods are presented, and computational effort and accuracy are discussed.

2.1.1 Finite element analysis of jacket support structures

It is common practice to analyze jacket support structures using beam finite element theory. Both 2-node Bernoulli-Euler and Timoshenko elements (Cook et al., 2002) are widely applied. Jackets are in general slender structures, hence the differences in the analyses using the two different beam formulations are very small. The beam elements have six degrees-of-freedom in each node, with a local element displacement vector $\boldsymbol{u}_e$ for all elements n_e given by:

$$\boldsymbol{u}_e = [u_x^1 \quad u_y^1 \quad u_z^1 \quad \theta_x^1 \quad \theta_y^1 \quad \theta_z^1 \quad u_x^2 \quad u_y^2 \quad u_z^2 \quad \theta_x^2 \quad \theta_y^2 \quad \theta_z^2]^T \tag{2.1}$$

The superscript refers to the node number, and u_x, u_y, u_z and $\theta_x, \theta_y, \theta_z$ are the displacements and rotations, respectively, see Fig. 2.1. The element stiffness matrix, $\boldsymbol{K}_e$, and consistent mass matrix, $\boldsymbol{M}_e$, are explicit functions of the design variables (diameters and thicknesses), and are in global coordinates given by:

$$\boldsymbol{K}_e(\boldsymbol{x}) = \int_{V_e} \boldsymbol{B}^T(\boldsymbol{x})\boldsymbol{E}\boldsymbol{B}(\boldsymbol{x})dV_e \tag{2.2}$$

$$\boldsymbol{M}_e(\boldsymbol{x}) = \int_{V_e} \rho_e \boldsymbol{N}^T(\boldsymbol{x})\boldsymbol{N}(\boldsymbol{x})dV_e \tag{2.3}$$

Here $\boldsymbol{B}$ is the strain-displacement matrix, $\boldsymbol{E}$ is the constitutive matrix, $\boldsymbol{N}$ contains the shape functions, ρ_e and V_e are the material density and volume for beam element e, respectively. By assembly over all n_e elements, the global stiffness matrix $\boldsymbol{K}$ and mass matrix $\boldsymbol{M}$ are obtained.

Structural damping can be included by assuming Rayleigh damping (also known as proportional damping). With this assumption, the damping matrix $\boldsymbol{C}$ can be described as:

$$\boldsymbol{C} = \alpha \boldsymbol{M} + \beta \boldsymbol{K} \tag{2.4}$$

The mass proportional α and stiffness proportional β parameters are determined by (Cook et al., 2002):

$$\xi = \frac{1}{2}\left(\frac{\alpha}{\omega} + \beta\omega\right) \tag{2.5}$$

Thus, the damping is a function of the structural frequency ω. By selecting a design spectrum between two known frequencies and choosing damping values at these two frequencies, the damping coefficients can be determined. Alternatively, the damping can be tuned at a single frequency, e.g. the first fore-aft frequency. To solve the above equation using only one frequency, the damping can be assumed to be at a minimum at the selected frequency. Thus, the derivative of the damping with respect to that frequency is zero.

Three approaches to modelling the fatigue are presented in this thesis, and the structural response is found differently for each of the methods:

$$\boldsymbol{M}(\boldsymbol{x})\ddot{\boldsymbol{u}}(\boldsymbol{x},t) + \boldsymbol{C}(\boldsymbol{x})\dot{\boldsymbol{u}}(\boldsymbol{x},t) + \boldsymbol{K}(\boldsymbol{x})\boldsymbol{u}(\boldsymbol{x},t) = \boldsymbol{P}(t) \qquad \text{(dynamic analysis)} \tag{2.6}$$

$$\boldsymbol{K}(\boldsymbol{x})\boldsymbol{u}(\boldsymbol{x},t) = \boldsymbol{P}(t) \qquad \text{(quasi-static analysis)} \tag{2.7}$$

$$\boldsymbol{K}(\boldsymbol{x})\boldsymbol{u}^{DEL}(\boldsymbol{x}) = \boldsymbol{P}^{DEL} \qquad \text{(static analysis)} \tag{2.8}$$

$\boldsymbol{P}$ is a time-history load corresponding to the time-dependent aerodynamic and hydrodynamic loading. The time-history load is used to construct the damage equivalent load $\boldsymbol{P}^{DEL}$. $\ddot{\boldsymbol{u}}$, $\dot{\boldsymbol{u}}$, and $\boldsymbol{u}$ are the vectors of structural acceleration, velocity and displacement, respectively, and $\boldsymbol{u}^{DEL}$ is the structural response to the DEL.

It is possible to include the soil-structure interaction in the finite element model in a variety of ways. However, for jackets for offshore wind turbines, the soil has only very little impact on the overall frequency, and the soil damping has practically no impact on the dynamic behavior or the fatigue (Seidel, 2014).

2.1.2 Loading conditions

In the verification of offshore support structures, many large Design Load Cases (DLC) must be applied. The load cases must represent a variety of situations of the turbine such as idling, operation, emergency stop etc. Additionally, the aerodynamic and hydrodynamic loading must represent everything from calm weather to extreme weather conditions with 50-years waves. In Table 2.1, a simplified overview of the load cases suggested by the offshore standard from DNV (2013) is shown. The proposed load cases are closely related to those from the onshore and offshore standard by IEC (2005, 2009).

A typical time-history load consists of ten minutes real time that is discretized into 30,000 load steps in the simulation. For a single load case, six of these ten minute time history loads for each relevant mean wind speed are required. Additionally, there may be variations in load direction, wave direction, yaw misalignment etc. Consequently, several thousand time-history loads are required in the verification of wind turbine components. A very limited amount of software can handle these very complicated and specialized numerical simulations. The numerical simulations are computationally very costly, and none of the state-of-the-art software perform simulations of detailed wind turbine models faster than real-time (Muskulus and Schafhirt, 2014).

Design situation	DLC	Wind condition	Wave condition	Wind and wave directionality	Other conditions	Type
Power production	1.1	NTM	NSS	Codirectional in one direction	For extrapolation of extreme events	ULS
	1.2	NTM	NSS	Codirectional in one direction		FLS
	1.3	ETM	NSS	Codirectional in one direction		ULS
	1.4	ECD	NSS	Misaligned		ULS
	1.5	EWS	NSS	Codirectional in one direction		ULS
	1.6a	NTM	SSS	Codirectional in one direction		ULS
	1.6b	NTM	SWH	Codirectional in one direction		ULS
Power production plus occurence of fault	2.1	NTM	NSS	Codirectional in one direction	Control system fault or loss of electrical connection	ULS
	2.2	NTM	NSS	Codirectional in one direction	Protection system fault or preceding internal electrical fault	ULS
	2.3a	EOG	NSS	Codirectional in one direction	External or internal electrical fault including loss of electrical network connection	ULS
	2.3b	NTM	NSS	Codirectional in one direction	External or internal electrical fault including loss of electrical network connection	ULS
	2.4	NTM	NSS	Codirectional in one direction	Control or protection system fault including loss of electrical network	FLS
Start up	3.1	NWP	NSS	Codirectional in one direction		FLS
	3.2	EOG	NSS	Codirectional in one direction		ULS
	3.3	EDC	NSS	Misaligned		ULS
Normal shutdown	4.1	NWP	NSS	Codirectional in one direction		FLS
	4.2	EOG	NSS	Codirectional in one direction		ULS
Emergency shutdown	5.1	NTM	NSS	Codirectional in one direction		ULS
Parked (standing still or idling)	6.1a	EWM	ESS	Misaligned multiple directions		ULS
	6.1b	EWM	RWH	Misaligned multiple directions		ULS
	6.1c	RWM	EWH	Misaligned multiple directions		ULS
	6.2a	EWM	ESS	Misaligned multiple directions	Loss of electrical network connection	ULS
	6.2b	EWM	RWH	Misaligned multiple directions	Loss of electrical network connection	ULS
	6.3a	EWM	ESS	Misaligned multiple directions	Extreme yaw-misalignment	ULS
	6.3b	EWM	RWH	Misaligned multiple directions	Extreme yaw-misalignment	ULS
	6.4	NTM	NSS	Codirectional in multiple directions	Extreme yaw-misalignment	FLS
Parked and fault conditions	7.1a	EWM	ESS	Misaligned multiple directions		ULS
	7.1b	EWM	RWH	Misaligned multiple directions		ULS
	7.1c	RWM	RWH	Misaligned multiple directions		ULS
	7.2	NTM	NSS	Codirectional in multiple directions		ULS

Table 2.1: Proposed various environmental conditions as given in DNV (2013). The table have been simplified. Abbreviations are: Normal Turbulence Model (NTM), Extreme Turbulence Model (ETM), Extreme Coherent gust with Direction change (ECD), Extreme Wind Shear (EWS), Extreme Operating Gust (EOG), Normal Wind Profile (NWP), Extreme Direction Change (EDC), Extreme Wind speed Model (EWM), Reduced Wind speed Model (RWM), Normal Sea State (NSS), Severe Sea State (SSS), Severe Wave Height (SWH), Extreme Sea State (ESS), Reduced Wave Height (RWH), and Extreme Wind Height (EWH).

The large amount of DLCs involved in the verification of a wind turbine component is currently much too large to handle in an optimization framework. In the very preliminary design phases of a jacket structure, it may be sufficient to include only DLC 1.2 for FLS purposes. This DLC represents the core loads a turbine is subjected to, i.e. the normal operational conditions. Normal operation for ULS can be represented by including DLC 1.3. DLC 6.1a and/or 6.1b are also considered very important for preliminary design. These DLCs are used to address a parked turbine subjected to extreme weather conditions.

In the following subsections the aerodynamic and hydrodynamic loading conditions in a state-of-the-art gradient based optimization framework will be described and discussed. Note that the loading condition is assumed fixed throughout the optimization. Thus, the design sensitivity analysis does not contain information on how the load changes with design changes. If the loading conditions are very sensitive to design changes, the optimization may provide poor and unrealistic designs. In Paper B an optimization of the cross sections of the OC4 reference jacket (Vorpahl et al., 2011) with the NREL 5 MW baseline turbine (Jonkman et al., 2009) showed that with a very large reduction in mass, the damage caused by the aerodynamic and hydrodynamic loadings did not change significantly when compared with initial design.

Aerodynamic loading

Aerodynamic loading is complicated to include in a gradient-based optimization framework. In state-of-the-art integrated time-domain simulation software, an aeroelastic simulation under inflow turbulence environment is performed. This is, however, not possible in finite element-based optimization software. Especially estimating the aeroelastic damping within an acceptable accuracy is complicated, as this is highly dependent on the movements of the blades (modeled using BEM). The following describes a method for producing a force and moment time-series that mimics the time-dependent aerodynamic loading and damping from the integrated analysis.

Initially, a full simulation of an RNA with dynamic inflow with a fixed boundary at the bottom of the RNA, corresponding to where it is mounted on the tower, is performed. The reaction forces and moments $\boldsymbol{f}_{\text{RNA}}$ in this clamped node are extracted. These types of loads are often applied directly in an optimization framework, but then the dynamics caused by the moving of the RNA is not accounted for. By performing two additional analyses these effects can be included.

An analysis without aerodynamics and using only the fixed rotor loads applied at tower top is performed. The displacements $\boldsymbol{u}_{\text{DC}}$ from this decoupled analysis are compared with displacements $\boldsymbol{u}_{\text{FC}}$ caused by a fully coupled aeroelastic integrated analysis. The differences in displacements $\boldsymbol{u} = \boldsymbol{u}_{\text{FC}} - \boldsymbol{u}_{\text{DC}}$ are then corrected for by applying corrective loads $\boldsymbol{f}_{\text{DeCon}}$ in addition to the fixed rotor loads. Ideally, a force and moment series $\boldsymbol{f}_{\text{RL}} = \boldsymbol{f}_{\text{DeCon}} + \boldsymbol{f}_{\text{RNA}}$ will then present the same displacements as a fully integrated analysis. The method of determining these loads is here described for a single degree-of-freedom system, but can be extended to multi degree-of-freedom systems (Passon and Branner, 2013). The process is sketched in Fig. 2.2.

The effect of a load $f(t)$ on a linear system at time $t = \tau$ can be thought of as the effect of an infinitesimal impulse load. For $t > \tau$, the response is:

$$du(t;\tau) = h(t-\tau)f(\tau)d\tau \tag{2.9}$$

$h(t)$ is the so-called Impulse Response Function (IRF). The response $u(t)$ is only supported for $[0;t]$, and can be determined by the Duhamel integral (Clough and Penzien,

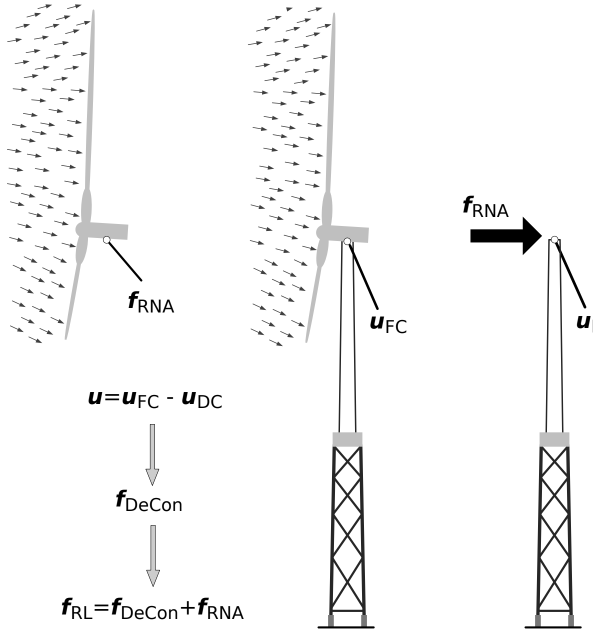

Fig. 2.2: The load generation process. Differences in displacements $\boldsymbol{u}$ from a fully coupled integrated analysis $\boldsymbol{u}_{\mathrm{FC}}$ and displacements from decoupled analysis $\boldsymbol{u}_{\mathrm{DC}}$ using fixed rotor loads $\boldsymbol{f}_{\mathrm{RNA}}$ are used to calculate a corrective force $\boldsymbol{f}_{\mathrm{DeCon}}$ using the deconvolution method. The rotor loads $\boldsymbol{f}_{\mathrm{RL}}$ are then the sum of the fixed rotor loads and the corrective loads.

1975):

$$u(t) = \int_0^t h(t-\tau) f(\tau) d\tau \tag{2.10}$$

$$u_n = \sum_{i=0}^{n-1} h_{n-i} f_i \, \Delta t \tag{2.11}$$

In the discretized expression, u_n is the displacement at time-step n, h the discretized IRF, f the discretized excitation, and Δt the time step. Using the convolution formula in an inverse manner, i.e. a deconvolution, gives the input force for a response. Thus, the discretized equation can be rewritten to present the force f_n at time step n:

$$f_n = \frac{1}{h_1} \left(\frac{u_n}{\Delta t} - \sum_{i=1}^{n-1} (h_{n+1-i} f_i) \right) \tag{2.12}$$

This equation is used directly to calculate the corrective force, f_{DeCon}. By this method, the aerodynamic damping is, in a way, included directly in the loading.

In the original work by Passon and Branner (2013), the method was not compared to state-of-the-art integrated analyses. However, in Paper B this comparison is made. In Fig. 2.3 the power spectral density of the displacement at tower top in wind direction for a low and high mean wind speed is shown for both the fully integrated state-of-the-art analysis, here performed using commercial software FEDEM Windpower

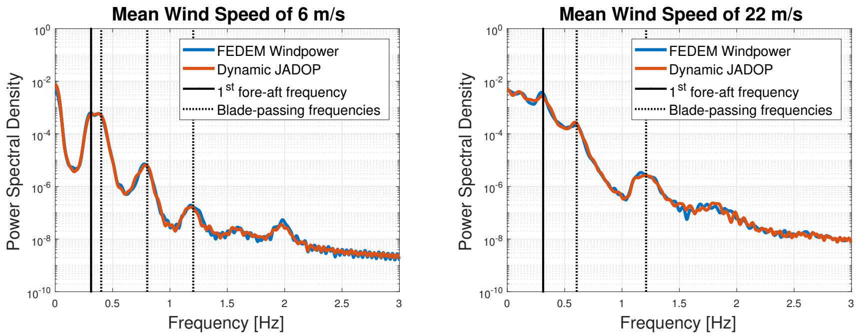

Fig. 2.3: Figure based on work from Paper B. Power spectral density of tower-top displacement in wind direction from a fully integrated analysis compared with an analysis using in-house software and deconvoluted rotor loads. Note that both structural frequencies and blade passing frequencies are captured correctly. The shown results are using the OC4 jacket and NREL 5 MW baseline turbine subjected to DLC 1.2.

(Fedem Technology AS, Trondheim, Norway, version R7.2.1), and using in-house software with deconvoluted tower-top loads determined using the described method. A very good match is observed. Small errors are expected as the simulations are not equal. For instance, Bernoulli-Euler beam elements and HHT Newmark-β time integration with $\alpha = 0.1$ are used in FEDEM Windpower. In the in-house software, Timoshenko beam elements and standard Newmark-β time integration are used.

Hydrodynamic loading

Hydrodynamic loading is a combination of wind-induced waves, which is a local phenomena, and swell, which are generated by distant weather systems. The sea state is determined by modeling of the sea surfaces and wave kinematics. The sea surface is characterized by a wave spectrum, e.g. the JONSWAP spectrum (Hasselmann et al., 1973). The kinematics can be computed using using linear wave theory. Linear wave kinematics only apply to the still water level. To extent the linear wave theory above still water level, Wheeler stretching (Wheeler, 1970) is applied. To model the waves, water depth, wave height, and wave period must be known. These values are typically determined by the metocean data, see e.g. Fischer et al. (2010) for an example of data.

Using the wave kinematics, the force exerted on the jacket members is determined using the Morison equation (Morison et al., 1950). For a fixed body, the force f_w is given by:

$$f_w = \rho_w C_m V \dot{u} + \frac{1}{2}\rho_w C_d A u|u| \tag{2.13}$$

ρ_w is the water density, C_m is the inertia coefficient, and C_d is the drag coefficient. $V = \frac{1}{4}\pi D^2$ is the volume of the body per unit cylinder length, and $A = D$ is area per unit cylinder length, with D being the outer diameter of the member. The water particle velocity u and acceleration $\dot{u}$ are perpendicular to the cylinder. This is not always true in a jacket structure, and the forces need to be reoriented. The tangential contributions are typically ignored.

The wave kinematics can vary significantly within the large space occupied by a jacket. Consequently, the wave kinematics at a time t is given for the part of the jacket that comes in contact with waves first. Then, other parts of the jacket are touched at a delayed time determined by the distance and the average wave velocity.

Note that if the diameter is not small compared with the wave-length, diffraction effects should be taken into account. This is primarily important for monopiles, and is therefore ignored in the present work.

In general, hydrodynamic loading does not contribute much to the structural response of jackets, and can be left out in FLS assessments during the early design phases (Seidel, 2014; Oest et al., 2017a).

Stress analysis

For linearly elastic conditions without prestress, the element stresses $\boldsymbol{\sigma}_e(\boldsymbol{u}(\boldsymbol{x},t),\boldsymbol{x})$ are obtained by:

$$\boldsymbol{\sigma}_e(\boldsymbol{u}_e(\boldsymbol{x},t),\boldsymbol{x}) = \boldsymbol{E}\boldsymbol{B}(\boldsymbol{x})\boldsymbol{u}_e(\boldsymbol{x},t) \tag{2.14}$$

The Det Norske Veritas recommended practice (DNV, 2014) suggests that all welded connections undergo a fatigue analysis. Welded connections contain high residual stresses caused by uneven contraction of the material during cooling. The residual stresses are difficult to determine. Moreover, two similar welds will often have different levels of residual stresses. For this reason, the recommended fatigue analysis disregard mean stress contributions. Additionally, as offshore support structures are highly dominated by normal stresses, shear stress contributions to the fatigue damage are neglected.

The most common fatigue assessment of jacket structures is using the so-called Hot Spot Stress (HSS) method. In the HSS method, a number of hotspots (typically eight) in the circumference of each welded connection are investigated. The increase in stresses in hot spots is due to changes in geometry in the welded connections. The HSS is not correctly captured by a beam finite element analysis, but can be estimated using Stress Concentration Factors (SCFs) applied to the nominal stresses. Thus, the SCFs are defined as the ratio between the nominal stress and the HSS.

The parametric SCFs for tubular joints recommended by DNV (2014) have been derived using 3D shell finite element analyses (Efthymiou and Durkin, 1985; Efthymiou, 1988). The SCFs are explicitly dependent on the design variables, and are also dependent on the connection type and the loading condition. Additionally, there are separate SCFs for each normal stress component. The nominal bending stresses in an element can be determined by:

$$[\sigma_e^{\mathrm{N}}(\boldsymbol{u}_e(\boldsymbol{x},t),\boldsymbol{x}) \quad \sigma_e^{\mathrm{MIP}}(\boldsymbol{u}_e(\boldsymbol{x},t),\boldsymbol{x}) \quad \sigma_e^{\mathrm{MOP}}(\boldsymbol{u}_e(\boldsymbol{x},t),\boldsymbol{x})]^T = \boldsymbol{E}\boldsymbol{B}_{xx}(\boldsymbol{x})\boldsymbol{u}_e(\boldsymbol{x},t) \tag{2.15}$$

Here $\boldsymbol{B}_{xx}$ is the strain-displacement matrix including only terms regarding normal stresses. The superscript indicates that the stress is caused by normal force (N), by in-plane bending (MIP), and by out-of-plane (MOP) bending. The eight hot spot locations are distributed as seen in Fig. 2.4. The HSS for location i is determined by

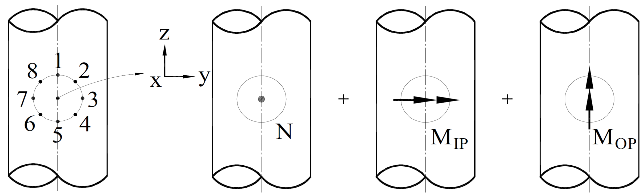

Fig. 2.4: Hot Spot Stresses in the circumference of a weld. Figure adapted from DNV (2014).

scaling each normal stress component with separate SCFs:

$$\sigma_i(\boldsymbol{u}_e(\boldsymbol{x},t),\boldsymbol{x}) = \begin{bmatrix} SCF_i^{\mathrm{N}}(\boldsymbol{x}) & SCF_i^{\mathrm{MIP}}(\boldsymbol{x}) & SCF_i^{\mathrm{MOP}}(\boldsymbol{x}) \end{bmatrix} \begin{bmatrix} \sigma_e^{\mathrm{N}}(\boldsymbol{u}_e(\boldsymbol{x},t),\boldsymbol{x}) \\ \sigma_e^{\mathrm{MIP}}(\boldsymbol{u}_e(\boldsymbol{x},t),\boldsymbol{x}) \\ \sigma_e^{\mathrm{MOP}}(\boldsymbol{u}_e(\boldsymbol{x},t),\boldsymbol{x}) \end{bmatrix} \tag{2.16}$$

These scaled stresses are used directly in the S-N-based fatigue analysis. To simplify the notation, the dependencies on the design variables $\boldsymbol{x}$ and state variables $\boldsymbol{u}$ will not be indicated in the rest of the section.

2.1.3 Fatigue limit state analysis

The recommended practice follows the typical approach to a stress-based high-cycle fatigue analysis. The fatigue analysis can be described by three subsequent steps:

1. Determine amplitude stresses from stress history using rainflow counting.
2. Relate stress amplitudes to expected number of cycles to failure using S-N data.
3. Accumulate all fractions of damage using Palmgren-Miner's rule.

The application of these procedures within a jacket optimization framework will be explained in the following.

Rainflow counting

Almost all engineering structures are subject to some form of variable amplitude loading. It is desirable to reduce the variable stress spectrum into stress amplitudes, which can be applied to a damage criterion. For this purpose, rainflow counting can be applied (Matsuishi and Endo, 1968). Rainflow counting consists of just a few steps, demonstrated in Fig. 2.5. A signal, e.g. a stress time-history, is reduced to peaks and valleys. From these peaks and valleys, the stress cycles are determined. The information provided by subjecting a stress spectrum to a rainflow counting algorithm is typically:

- Stress amplitude
- Stress mean
- Number of cycles (half or full)
- Begin time of cycle
- Period of cycle

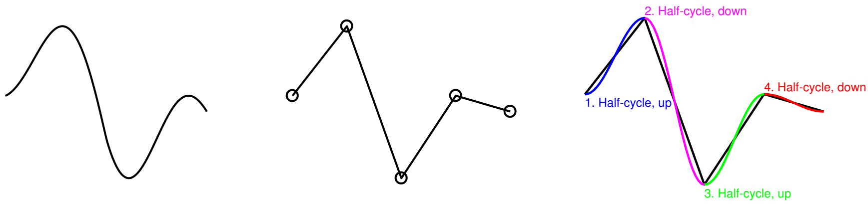

(a) (b) (c)

Fig. 2.5: **(a)** A variable amplitude signal is given to to the rainflow counting algorithm. **(b)** Peaks and vallyes are identified. **(c)** Cycles are identified from the peaks and valleys.

The stress amplitude, stress mean, and number of cycles are directly applicable to many stress-based fatigue criteria. The begin time of a cycle and the period of a cycle are important in the design sensitivity analysis, such that the correct displacement sensitivities can be calculated to a corresponding stress cycle. This is further explained in Section 2.1.6.

A great feature of rainflow counting is that it allows for the application of S-N data and cumulative fatigue laws. Note that traditional rainflow counting algorithms do not take into account the sequence of loading. Additionally, they process just one signal at a time (e.g. normal stress or a reference stress such as the von Mises stress).

S-N relations

S-N relations are used to relate a stress range (or stress amplitude) to an expected number of cycles to failure. Typically, S-N curves are derived by fatigue tests of relatively small specimens, where the majority of the fatigue life is associated with crack growth. However, tests of tubular joints are typically of larger sizes where redistribution of stresses during crack growth is possible. In the test of tubular joints, the crack can grow both through the thickness but also along the joint before fracture occurs. The applied S-N curves are from DNV (2014), where the number of cycles are determined by through-thickness cracks. The S-N relation is given by:

$$\log N_{ij} = \log\bar{a} - m\log\Delta\sigma_{ij} \tag{2.17}$$

N_{ij} is the estimated cycles to failure for location i and stress cycle j. m is the negative inverse slope of the S-N curve, and $\log\bar{a}$ is the intercept of the $\log N$-axis of the S-N curve. The S-N curves are based on the mean minus two standard deviation curves of the Gaussian distribution and are therefore predicting a 97.7% probability of survival. Thus:

$$\log\bar{a} = \log a - 2s_{\log N} \tag{2.18}$$

$\log a$ is the intercept of the mean S-N curve with the $\log N$-axis and $s_{\log N}$ is the standard deviation of $\log N$. The thickness of a plate can influence the fatigue strength of a welded joint, and can be accounted for by a thickness correction term on the S-N data:

$$\log N_{ij} = \log\bar{a} - m\log\left(\Delta\sigma_{ij}\left(\frac{t}{t_{\text{ref}}}\right)^k\right) \tag{2.19}$$

Here t is the thickness, t_{ref} is the reference thickness, and k is the thickness exponent. If all steel is assumed submerged in seawater, the applied S-N data for tubular joints is given as:

$$t = \max(t, t_{\text{ref}}) \qquad k = \begin{cases} 0.25, & \text{if } SCF \leq 10.0 \\ 0.30, & \text{otherwise.} \end{cases}$$

$$\log\bar{a} = \begin{cases} 11.764, & \text{if } \Delta\sigma_{ij} \geq 83.41MPa \\ 15.606, & \text{otherwise.} \end{cases} \qquad m = \begin{cases} 3.0, & \text{if } \Delta\sigma_{ij} \geq 83.41MPa \\ 5.0, & \text{otherwise.} \end{cases} \tag{2.20}$$

The above values are valid for cathodic protected steel with a yield strength up to 550 MPa. For more details on S-N curves for offshore steel structures, see DNV (2014). The estimated cycles to failure N_{ij} as determined by the S-N data allows for direct use of cumulative damage laws.

Cumulative laws

The recommended practice suggests to apply the most well-known cumulative law, i.e. Palmgren-Miner's linear damage hypothesis (also referred to as Palmgren-Miner's rule or Miner's rule) developed by Palmgren (1924) and made popular by Miner (1945). The rule states that the accumulated damage, D_i, in location i can be estimated by:

$$D_i = \sum_{j=1}^{n_j} \frac{n_{ij}}{N_{ij}} \leq \eta \tag{2.21}$$

Here n_{ij} is the number of cycles for the stress state $j = 1, ..., n_j$. When the accumulated damage reaches a design value η, typical set as $\eta = 1$, fatigue failure is expected to occur. The above equation can be applied directly as a finite-life fatigue constraint.

Palmgren-Miner's rule does not account for several factors known to influence the fatigue life. For instance, load sequence and interaction effects are not accounted for in the damage rule. Although many non-linear damage models have been developed, they are not necessarily able to correctly capture the many complicating factors influencing fatigue life. Therefore, linear damage rules are still dominantly applied in fatigue analysis of metals (Stephens et al., 2000; Fatemi and Shamsaei, 2011).

In a fatigue analysis, it is common practice to only use loading data corresponding to a fraction of the lifetime. The fatigue damage is then extrapolated to represent the lifetime of the structure. In wind energy, a series of loads of $n_S = 600$ s are typically used for this purpose. Let c_k be a scaling factor used to scale the damage to represent the full life time and $k = 1, ..., n_k$ be the amount of load time-series. Then the accumulated damage can be estimated by:

$$D_i = \sum_{k=1}^{n_k} c_k \sum_{j=1}^{n_j} \frac{n_{ijk}}{N_{ijk}} \leq \eta \tag{2.22}$$

The DEL method was originally developed by NREL and described in the work by Freebury and Musial (2000). The DEL approach does not contain a time-varying non-proportional load spectrum. Instead, a harmonic load of 1 Hz and range of $\Delta \boldsymbol{P}^{1\text{Hz}}$ is applied. Let D_i be the original accumulated damage as described above, and D_i^{DEL} be the accumulated damage caused by the damage equivalent load:

$$D_i = \sum_{k=1}^{n_k} c_k \sum_{j=1}^{n_j} \frac{n_{ijk}}{N_{ijk}} \qquad \frac{1}{N_{ijk}} = \frac{\left(\Delta\sigma_{ijk}\right)^m}{\bar{a}} \tag{2.23}$$

$$D_i^{\text{DEL}} = \frac{n_T}{N_i^{1\text{Hz}}} \qquad \frac{1}{N_i^{1\text{Hz}}} = \frac{\left(\Delta\sigma_i^{\text{DEL}}\right)^m}{\bar{a}} \tag{2.24}$$

Here $n_T = \sum_{k=1}^{n_k} c_k n_S$ is the total lifetime of the jacket, and $\Delta\sigma_i^{\text{DEL}}$ is the stress range caused by the DEL in location i. If one degree-of-freedom loading and quasi-static modeling are assumed, then there is a linear relationship between the loading history and the stress history, $\sigma_i = \alpha_i \boldsymbol{P}(t)$. Setting $D_i = D_i^{DEL}$, the DEL can be determined:

$$\frac{n_T(\alpha_i \Delta \boldsymbol{P}^{1\text{Hz}})^m}{\bar{a}} = \sum_{k=1}^{n_k} c_k \sum_{j=1}^{n_j} \frac{n_{jk}\left(\alpha_i \Delta \boldsymbol{P}_{jk}\right)^m}{\bar{a}} \tag{2.25}$$

$$\Rightarrow \Delta \boldsymbol{P}^{1\text{Hz}} = \left(\frac{1}{n_T} \sum_{k=1}^{n_k} c_k \sum_{j=1}^{n_j} n_{jk} \left(\Delta \boldsymbol{P}_{jk}\right)^m\right)^{\frac{1}{m}} \tag{2.26}$$

As the time-varying loading has been reformulated into a static load, the accumulated fatigue constraint can also be reformulated into a static stress constraint. The DEL fatigue constraint, written as a stress-based problem, is:

$$-\bar{\sigma} \leq \sigma_i^{\text{DEL}} \leq \bar{\sigma}, \qquad \bar{\sigma} = \left(\frac{\eta \bar{a}}{n_T}\right)^{\frac{1}{m}}, \qquad \forall i \tag{2.27}$$

It is only possible to include a linear S-N curve in the DEL method. Thus, it is up to the designer which of the material values in (2.20) to apply, or if an interpolation of the two should be applied.

2.1.4 Ultimate limit state analysis

Ultimate Limit State (ULS) constraints can have a large influence on the design of jacket structures. In optimization of jacket structures, the typical ULS constraints addressed are material yield limits and structural strength constraints, i.e. buckling. Common for all ULS constraints is that they must be satisfied in many places, for every load-step, and in all ULS load series. Consequently, for even small models and a limited number of load series, millions of ULS constraints exist.

Generally, the very large number of constraints can be addressed using active set strategies (also referred to as active set method and constraint lumping). In active set strategies, only the most important constraints are included in the optimization problem. A typical optimization problem with extremely many constraints will at the optimum have a much smaller number of active constraints than total number of constraints.

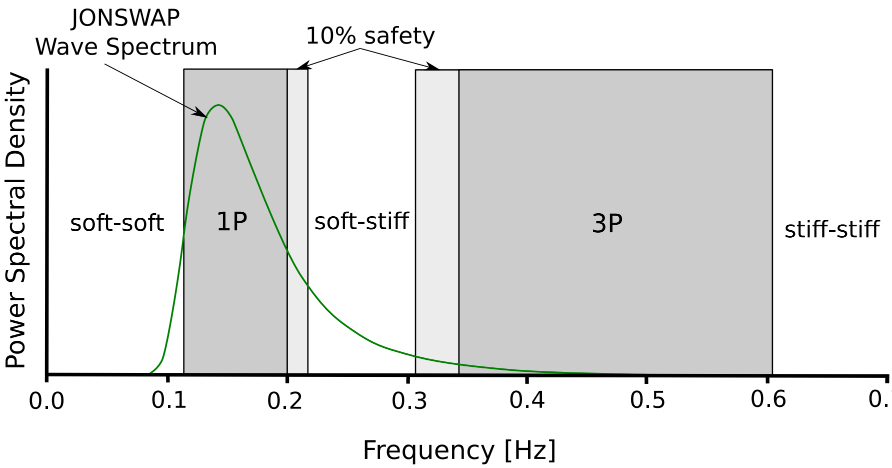

Fig. 2.6: Frequency plot showing the soft-stiff region with a ten percent margin on frequencies, demonstrated here on the NREL 5 MW reference turbine. Figure based on Fischer et al. (2010).

2.1.5 Frequency analysis

The first natural frequencies of offshore wind turbine structures are designed within one of three frequency bands, commonly referred to as either soft-soft, soft-stiff, or stiff-stiff. The three frequency bands are divided by the rotor frequency (1P), and the blade passing frequency (3P, also referred to as blade shadowing frequency) bands. In other words, the soft-soft design is below the 1P frequency band, the soft-stiff between the 1P and 3P frequency bands, and the stiff-stiff above the 3P frequency band. Typically, the soft-soft design is reserved to compliant designs, such as floating offshore wind turbines, where the soft-stiff and stiff-stiff designs are used in bottom-fixed rigid structures. A jacket is typically designed in the soft-stiff region, and with a ten percent safety margin, see Fig. 2.6.

In a jacket optimization framework, the first fore-aft frequency and first side-to-side frequency should be constrained to lie within the soft-stiff region. When optimizing jackets modeled with beam finite elements, the computational cost associated with the frequency analysis is negligible as compared with a FLS or ULS analysis.

2.1.6 Design sensitivity analysis

The following section presents the Design Sensitivity Analysis (DSA) of the fatigue constraints for each of the three approaches, i.e. DEL, quasi-static modeling, and dynamic modeling. For an overview of DSA methods, see Tortorelli and Michaleris (1994).

Generally, there are two approaches to analytical design sensitivity analyses. There is the direct differentiation method and there is the adjoint method. The direct differentiation method requires a solution of one pseudo problem for each design variable. The adjoint method requires a solution to one adjoint problem for each constraint function. In short, the direct differentiation method is generally the most efficient method for optimization problems with fewer design variables than constraints.

DSA - Damage Equivalent Loads

In Paper B, the DSA of the DEL-approach is performed using the direct differentiation method. Differentiating the constraint equation as defined in (2.27) with respect to a design variable x_v gives:

$$\frac{d\sigma_i^{\text{DEL}}}{dx_v} = \frac{\partial \sigma_i^{\text{DEL}}}{\partial x_v} + \frac{\partial \sigma_i^{\text{DEL}}}{\partial \boldsymbol{u}^{\text{DEL}}} \frac{d\boldsymbol{u}^{\text{DEL}}}{dx_v} \tag{2.28}$$

The partial derivatives are computationally inexpensive. The displacement sensitivity is found by differentiating the global equilibrium equation (2.8) with respect to a design variable:

$$\boldsymbol{K} \frac{d\boldsymbol{u}^{\text{DEL}}}{dx_v} = -\frac{d\boldsymbol{K}}{dx_v} \boldsymbol{u}^{\text{DEL}} \tag{2.29}$$

The derivative of the applied load vector with respect to the design variable has vanished since the loads are assumed fixed. This equation only needs to be solved for each design variable. In jacket sizing optimization the number of design variables is typically around 20. As the amount of constraints for sizing optimization is much larger than the amount of design variables, an adjoint formulation is less effective for this problem. However, using adjoint formulations in combination with aggregation functions are very effective. This is further discussed in Section 2.2.2.

DSA - Quasi-static

The constraint equation used in both the quasi-static and dynamic approaches is Palmgren-Miner's rule (2.22). Using the direct differentiation method and differentiating Palmgren-Miner's rule with respect to a design variable, the sensitivity is obtained as:

$$\frac{dD_i}{dx_v} = \frac{\partial D_i}{\partial x_v} + \sum_{k=1}^{n_k} \sum_{j=1}^{n_j} \frac{\partial D_{ijk}}{\partial \Delta \boldsymbol{u}_{jk}} \frac{d\Delta \boldsymbol{u}_{jk}}{dx_v} \tag{2.30}$$

To determine the displacement sensitivities, (2.7) is differentiated with respect to a design variable:

$$\boldsymbol{K} \frac{d\Delta \boldsymbol{u}_{jk}}{dx_v} = -\frac{d\boldsymbol{K}}{dx_v} \Delta \boldsymbol{u}_{jk} \tag{2.31}$$

This equation needs to be solved for every displacement range $\Delta \boldsymbol{u}_{jk}$ and for each design variable. Thus, it is significantly more costly than the DEL approach. The correct displacement range $\Delta \boldsymbol{u}_{jk}$ can be found by using the information provided by the rainflow counting algorithm, i.e. the begin time of the stress cycle and the period of the stress cycle. The above formulation is demonstrated in Paper B.

In Paper A, an efficient adjoint formulation of fatigue constraints in jacket structures is presented, where the number of adjoint equations is independent of load cycles due to linear relations. Thus, a reference adjoint equation is solved for each constraint i:

$$\boldsymbol{K} \boldsymbol{\lambda}_i^{\text{ref}} = \frac{\partial \Delta \sigma_i}{\partial \Delta \boldsymbol{u}} \tag{2.32}$$

In this equation, there is no subscript jk as this partial derivative does not depend on the stress cycles. The real adjoint vector for a given stress range (or amplitude) is then recovered by linear scaling:

$$\boldsymbol{\lambda}_{ijk} = \frac{\partial D_{ijk}}{\partial \Delta\sigma_{ijk}} \boldsymbol{\lambda}_i^{\text{ref}} \tag{2.33}$$

Here D_{ijk} and $\Delta\sigma_{ijk}$ are the damage and stress ranges in location i for cycle j in load case k. The design sensitivity is obtained by:

$$\frac{dD_i}{dx_v} = \sum_{k=1}^{n_k} \sum_{j=1}^{n_j} \frac{\partial D_{ijk}}{\partial x_v} - \boldsymbol{\lambda}_{ijk}^T \frac{d\boldsymbol{K}}{dx_v} \Delta \boldsymbol{u}_{jk} \tag{2.34}$$

Note that in Paper B, it was demonstrated that quasi-static modeling approaches (and thus also DEL) may severely underestimate the fatigue damage. Naturally, when using quasi-static methods it is important that structural frequencies are not excited in such a manner, that they contribute significantly to the overall fatigue damage. Otherwise, appropriate safety factors should be applied to the fatigue constraint in the optimization. In Paper B a simple safety factor is proposed that worked well within the framework.

DSA - Dynamic

The equation for the fatigue design sensitivities in the dynamic approach is the same as the quasi-static approach, i.e. (2.30). However, the computation of the derivative of the displacement range differs. The displacement sensitivity in the dynamic approach is found by the direct differentiation method. Differentiating (2.6) with respect to a design variable, the displacement sensitivity is obtained as:

$$\boldsymbol{K}\frac{d\Delta \boldsymbol{u}_{jk}}{dx_v} = -\frac{d\boldsymbol{M}}{dx_v}\Delta\ddot{\boldsymbol{u}} - \boldsymbol{M}\frac{d\Delta\ddot{\boldsymbol{u}}_{jk}}{dx_v} - \frac{d\boldsymbol{C}}{dx_v}\Delta\dot{\boldsymbol{u}} - \boldsymbol{C}\frac{d\Delta\dot{\boldsymbol{u}}_{jk}}{dx_v} - \frac{d\boldsymbol{K}}{dx_v}\Delta\boldsymbol{u}_{jk} \tag{2.35}$$

This equation is more computationally expensive than the quasi-static counterpart. It does not allow for direct computation as the displacements are time dependent. Thus, time integration is necessary. A common approach is to solve for all displacement derivatives for all time steps using Newmark time integration. The displacement range sensitivity, $\frac{d\Delta \boldsymbol{u}_{jk}}{dx_v}$, can be found by subtracting two displacement derivatives from each other, where the locations in time of the two displacement derivatives are determined by the rainflow counting algorithm. For large load series and many degrees-of-freedom the computational costs may become very large, and memory may become an issue. The above approach is based on the work by Chew et al. (2015); Chew (2017) and evaluated in Paper B. An efficient analytical adjoint approach to design sensitivity analysis has, to the authors knowledge, not yet been demonstrated for sizing optimization of jacket structures using a dynamic analysis. The above methods are described for sizing optimization of jacket structures, but are of a general nature. Next, focus is on topology optimization with fatigue constraints.

2.2 Topology optimization with fatigue constraints

This brief state-of-the-art section is split intro three parts: (i) classical density-based topology optimization, (ii) stress-based topology optimization, and (iii) fatigue-based topology optimization. Note that only density-based topology optimization will be covered. Other approaches to solving the topology problem such as level-set, topological derivative, phase field, evolutionary etc. will not be covered. For comprehensive reviews of the topology optimization method, see Bendsøe and Sigmund (2004); Rozvany (2009); Sigmund and Maute (2013); Deaton and Grandhi (2014).

2.2.1 Topology optimization

The aim of classical topology optimization is to find an optimal material distribution. The typical approach is to discretize the design space with finite elements, and then assign each finite element a design variable, x_e, stating if there is material or if there is no material (void) in the given element. The desired design is referred to as a black and white design, with black indicating material and white indicating void. See Fig. 2.7 for an example of topology optimization. The black and white parameterization can be defined as:

$$x_e = \begin{cases} 1 & \text{if material in element } e \\ 0 & \text{if void} \end{cases} \tag{2.36}$$

The majority of works with structural topology optimization is using a linear elastic finite element analysis. In the analysis, void regions must not contribute to the stiffness and mass of the overall structure. Thus:

$$E_e = x_e E_0 \tag{2.37}$$

$$m_e = x_e \rho V_e \tag{2.38}$$

$$x_e \in \{0;1\}, \quad \forall e$$

Here E_e is the effective Young's modulus for element e. E_0 is the stiffness for full material density, m_e is the mass of element e, ρ is the material density, and V_e is

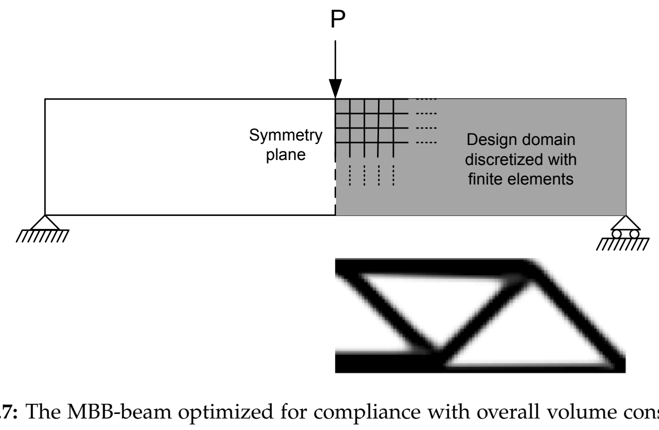

Fig. 2.7: The MBB-beam optimized for compliance with overall volume constraint.

the volume of element e. It is well-known that integer programming problems with many design variables are difficult to solve. Thus Bendsøe (1989) developed the well-known SIMP (Solid Isotropic Material with Penalization, also referred to as Solid Isotropic Microstructure with Penalization) interpolation scheme, that reformulates the discrete variables into continuous variables. Thus, the effective Young's modulus of elasticity can be formulated by:

$$E_e = x_e^p E_0 \tag{2.39}$$

$$m_e = x_e \rho V_e \tag{2.40}$$

$$x_e \in]0;1], \quad \forall e$$

The interpolation parameter $p > 1$ ensures that intermediate densities provide too compliant designs as compared with the linearly interpolated mass. However, this formulation does not allow the design variables to have a zero value. To allow for zero densities, the modified SIMP interpolation scheme can be applied:

$$E_e = E_{min} + x_e^p (E_0 - E_{min}) \tag{2.41}$$

$$x_e \in [0;1], \quad \forall e$$

Here $E_{min} \ll E_0$ is a lower bound on the void material stiffness. Note that many other material interpolation schemes exist, see e.g. Bendsøe and Sigmund (1999); Stolpe and Svanberg (2001a). Using the modified SIMP, a singular stiffness matrix is avoided for zero densities. However, the large difference in stiffness of solid and void material makes the linear system ill-conditioned, which can lead to inaccuracies and slower convergence (Wang et al., 2007). The modified SIMP formulation allows for easy implementation of filters.

Restriction methods, such as density filtering, are introduced since the original topology problem can produce so-called checkerboards that contain an artificial high stiffness, see Fig. 2.8. Additionally, the solution to the topology problem is mesh-dependent. Mesh-dependency is a direct result of the lack of existence of solutions of the original discrete topology problem. To ensure mesh independence and increase manufacturability in density-based topology optimization, many different approaches can be applied. One of the most popular approaches is to apply the consistent density filter (Bourdin, 2001; Bruns and Tortorelli, 2001). The filtering technique is both easy to implement and computationally efficient. The density filter alters the problem by including a weighted average of the densities in neighboring elements. The amount of elements included is set by a user-specified radius and effectively also works as a minimum length scale parameter. The filtered problem enters directly into the physics, and the filtered densities are therefore often referred to as physical variables.

Fig. 2.8: An MBB-beam optimized for compliance suffering from the so-called checkerboards.

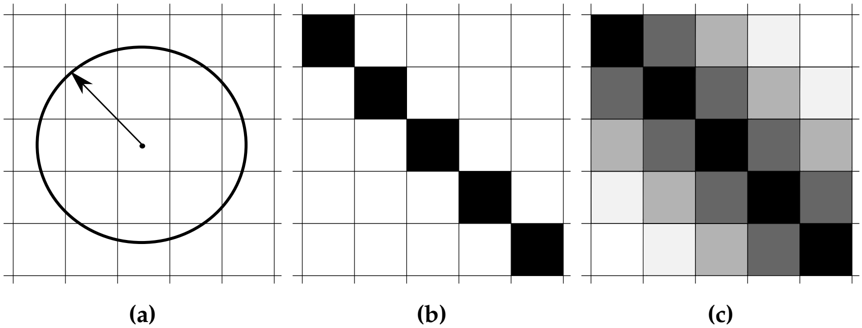

Fig. 2.9: **(a)** A radius on the structured mesh defines how many neighboring elements to include in the filtering process. **(b)** An unfiltered mesh with the so-called checkerboard problem. **(c)** The filtered (physical) mesh of the checkerboard problem in **(b)**. A decaying weight function assigns less density to elements furthest away from the center of the filter. Note that using the density filter will always result in grayscale unless special techniques are applied.

See Fig. 2.9 for a graphical explanation of density filtering. For more literature on restriction methods, see e.g. Sigmund and Petersson (1998); Sigmund (2007).

Topology optimization has been applied to various fields including complex multiphysics problems. However, most work has been done on minimizing the compliance subject to an overall mass (or volume) constraint. This problem can be written as:

$$\begin{aligned} \min_{\boldsymbol{x}\in X}. \quad & f(\boldsymbol{x}) = \boldsymbol{P}^T \boldsymbol{u}(\boldsymbol{x}) \\ \text{s.t.} \quad & \boldsymbol{K}(\boldsymbol{x})\boldsymbol{u}(\boldsymbol{x}) - \boldsymbol{P} = \boldsymbol{0} \\ & g(\boldsymbol{x}) = \sum_{e=1}^{n_e} x_e \rho V_e \leq \bar{m} \end{aligned} \tag{2.42}$$

Here $X = \{\boldsymbol{x} \in \mathbb{R}^e |\ 0 \leq x_e \leq 1, e = 1, \ldots, n_e\}$, n_e being the total number of elements and $\bar{m}$ being the upper limit on the mass. Note that the loading condition is assumed design independent. The minimization of compliance is a convenient problem to solve as compliance is a global measure representing the entire structure, and the design sensitivity is computationally inexpensive due to the self-adjoint nature of the problem. On the other hand, stress and fatigue are local quantities, which introduce additional difficulties in the topology optimization. However, stress and fatigue are much more common design criteria as compared with compliance.

2.2.2 Stress-based topology optimization

The stress-constrained topology optimization problem is often formulated as minimization of mass constrained by a stress limit, $\bar{\sigma}$, in every element. The optimization problem can be written as:

$$\begin{aligned} \min_{x \in X} \quad & f(\boldsymbol{x}) = \sum_{e=1}^{n_e} x_e \rho V_e \\ \text{s.t.} \quad & \boldsymbol{K}(\boldsymbol{x})\boldsymbol{u}(\boldsymbol{x}) - \boldsymbol{P} = \boldsymbol{0} \\ & g_e(\boldsymbol{x}) = \frac{\sigma_e(\boldsymbol{x}, \boldsymbol{u}(\boldsymbol{x}))}{\bar{\sigma}} - 1 \leq 0, \quad \forall e \end{aligned} \tag{2.43}$$

Here σ_e is the element stress, where it is assumed that the stress is only evaluated in one location per element, which is the common practice in stress-based optimization. Typically, the von Mises stress is used, but any reference stress or stress component can be applied. The Drucker-Prager yield criterion, which is a pressure-dependent criterion, has also been applied in many works.

The stress-based optimization problem introduces new difficulties that must be addressed. Especially, how to determine stresses for intermediate densities, how to address singular optima, and how to handle the large number of constraints are difficult problems.

Interpolation of stresses

In Duysinx and Sigmund (1998); Duysinx and Bendsøe (1998) interpolation of stresses in stress-based topology optimization is investigated by studying the microscopic stresses in a layered composite (rank 2 material). Their method ensures physical consistency of stresses not only for 0-1 designs, but also for designs with intermediate densities.

In the following, assume that an intermediate density represents a porous microstructure, and that SIMP provides the effective stiffness of that microstructure. Then, the macroscopic stress $\langle \sigma_e \rangle$, is given by the effective material properties of the microstructure using SIMP:

$$\langle \sigma_e \rangle = \boldsymbol{S}_e(E_e)\boldsymbol{u}_e = x_e^p \boldsymbol{S}_e(E_0)\boldsymbol{u}_e \tag{2.44}$$

Here $\boldsymbol{S}_e$ is the stress-displacement matrix and $\boldsymbol{u}_e$ is the element displacement vector. The formulation of macroscopic stresses is invariant to changes in the design variable. This is true as multiplying the density with a constant $\alpha < 1$ increases the displacements by $\frac{1}{\alpha^p}$, but the stresses are reduced with the factor α^p. Consequently, using this formulation in minimization of mass topology optimization will generally lead to removal of all material (Verbart, 2015). Therefore, using the macroscopic stresses is not a suitable formulation for topology optimization. Hence, the authors presented a method based on the microscopic stresses.

The microscopic stress in rank 2 material is inverse proportional to the density, and is given by:

$$\sigma_e = \frac{\langle \sigma_e \rangle}{x^q} = \frac{x_e^p}{x_e^q} \boldsymbol{S}_e(E_0)\boldsymbol{u}_e \tag{2.45}$$

For $q = p$, the microscopic stress is finite and non-zero when the density is zero. This is physical consistent with a rank 2 material. However, the non-zero stress at zero densities leads to singular optima.

Singular optima and relaxation methods

A well-known issue with stress-based optimization is the so-called singular optima (also referred to as the singularity problem) which were discovered in stress-based optimization of truss structures in the 1960's (Sved and Ginos, 1968). A three-bar problem was investigated, and the true optimum was a two bar solution. However, the two-bar solution is unreachable by standard non-linear programming because the stress constraint prevents the bar from vanishing. The singular optima are belonging to degenerate subspaces of lower dimensions (Kirsch, 1990).

In order to avoid degenerate subspaces, the stress-constrained topology optimization problem is often reformulated using a relaxation technique. The two most well-known relaxation methods are the ϵ-relaxation and the qp-relaxation. Many variations of both methods have been proposed.

Using the ϵ-relaxation (Cheng and Guo, 1997; Duysinx and Bendsøe, 1998; Verbart, 2015), the stress-based optimization problem defined in (2.43) is reformulated:

$$\begin{aligned} \min_{\boldsymbol{x}\in X} \quad & f(\boldsymbol{x}) = \sum_{e=1}^{n_e} x_e \rho V_e \\ \text{s.t.} \quad & \boldsymbol{K}(\boldsymbol{x})\boldsymbol{u}(\boldsymbol{x}) - \boldsymbol{P} = \boldsymbol{0} \\ & \bar{g}_e(\boldsymbol{x}) = g_e(\boldsymbol{x}) - \epsilon \leq 0, \quad \forall e \end{aligned} \tag{2.46}$$

Here $0 < \epsilon \ll 1$ is a relaxation parameter that perturbs the design space such that it no longer contains degenerate parts. The ϵ value is typically continuously decreased during the optimization. This may lead to convergence to the global optimum, but it is not a guarantee (Stolpe and Svanberg, 2001b).

The qp-relaxation method proposed in Bruggi and Duysinx (2012) introduces zero stresses at zero densities in the formulation of microscopic stress given in (2.45):

$$\boldsymbol{\sigma}_e = x_e^{p-q} \boldsymbol{S}_e(E_0)\boldsymbol{u}_e, \quad q < p \tag{2.47}$$

With this formulation, intermediate densities no longer have a physical interpretation (as $q \neq p$). The formulation relaxes the design space. However, as with ϵ-relaxation, a global optimum is not guaranteed. It should be noted that an advantage of this method is that for any zero-one design, the constraint is actually satisfied, which is not true for ϵ-relaxation if $\epsilon > 0$.

A popular relaxation method in stress-based topology optimization is the so-called relaxed stress formulation, which is a qp-based formulation, and is described in Le et al. (2010). The difference as compared with the original qp-relaxation is that the relaxed stress is also used to interpret the optimized design, and it is therefore no longer a strictly mathematical operation (Verbart, 2015).

Local constraints

In stress constrained topology optimization, it is common practice to evaluate the stress-level in the centroid of each finite element. When the amount of constraints equals the amount of design variables, the design sensitivity analysis becomes computational expensive as the efficiency of the adjoint method is lost

(Tortorelli and Michaleris, 1994). Several works exist where stress optimization has been performed considering each stress evaluation as a local constraint, see e.g. Navarrina et al. (2005); Bruggi (2008); Bruggi and Venini (2008).

There exist three popular approaches to address the large amount of constraints.

The first approach is the active set method, as explained in section 2.1.4. However, the aim of stress constrained topology optimization is to achieve a fully stressed design where all elements with full density have an active or near active stress constraint. Thus, the amount of constraints in the active set may become very large for a fine finite element discretization. The active set method has been applied successfully to stress-based topology optimization in e.g. Duysinx and Bendsøe (1998); Bruggi and Duysinx (2012); Luo et al. (2013a); Bruggi and Duysinx (2013).

The second approach is the augmented Lagrangian method (also called the multiplier method). In the augmented Lagrangian method, the constrained optimization problem is reformulated into an unconstrained problem by adding a penalty term to the Lagrangian of the problem. Every constraint equation adds one Lagrange multiplier and one penalty parameter. Thus, the size of the problem increases, but only one system of linear equations per load case needs to be evaluated to determine the adjoint vector. For an overview of this method, see e.g. Arora et al. (1991), and for an implementation in a topology framework for stress constrained problems, see e.g. Pereira et al. (2004); da Silva et al. (2017).

The third and most common approach in topology optimization is using aggregation functions. Aggregation functions group all (or some) constraint functions into an approximation (aggregation) function. Thus, a problem with a large number of constraints can be reduced to a more convenient number of constraints.

Many aggregation functions exist. Two of the most popular functions are shown below. The first equation is the Kreisselmeier-Steinhauser (KS) function (Kreisselmeier and Steinhauser, 1980) g^{KS} and the second equation is the P-norm function g^{PN}:

$$g^{\mathrm{KS}}(\boldsymbol{x}) = \frac{1}{P}\ln\left(\sum_{e=1}^{n_e} e^{P g_e(\boldsymbol{x})}\right) \tag{2.48}$$

$$g^{\mathrm{PN}}(\boldsymbol{x}) = \left(\sum_{e=1}^{n_e} g_e(\boldsymbol{x})^P\right)^{\frac{1}{P}} \tag{2.49}$$

The parameter $P \geq 1$ will for larger values present a better representation of the highest function value, see Fig. 2.10. However, increasing the parameter makes the equation increasingly non-linear which can lead to numerical problems during optimization. Thus, it is a tuning parameter that varies in value depending on the application. In a stress-based topology setting, the accuracy of the aggregation function is mesh-dependent. To properly capture the stress field a fine mesh is required. However, increasing the mesh resolution without increasing the number of aggregation functions will make each aggregation function less accurate, as it needs to represent more function values. The KS function has been applied to density-based stress optimization in Yang and Chen (1996); París et al. (2009, 2010); Luo and Kang (2012); Luo et al. (2013b). In Yang and Chen (1996); Duysinx and Sigmund (1998); Le et al. (2010); Jeong et al. (2012); Lee et al. (2012); Holmberg et al. (2013); Lian et al. (2017)

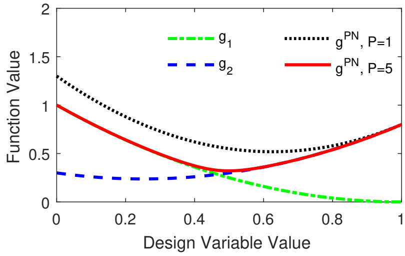

(a) P-norm aggregation function.

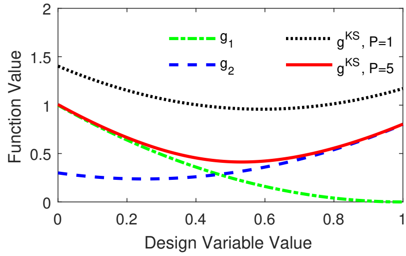

(b) KS aggregation function.

Fig. 2.10: Two aggregation functions with two different aggregation parameters

the P-norm method is used.

To make the optimization problem easier to solve, it is desirable to have a low aggregation function parameter. However, this often results in a poor approximation. To address this, an efficient method to adaptively scale the aggregation function towards the highest true constraint function value is proposed in Le et al. (2010). Applied on a P-norm function, the scaled constraint function $\bar{g}$ is in each iteration (I) given by:

$$\bar{g}(\boldsymbol{x}^{(I)}) = c^{(I)} g^{\text{PN}}(\boldsymbol{x}^{(I)}) \tag{2.50}$$

The scaled constraint function is a close approximation of the highest true constraint function value. The adaptive constraint scaling factor $c^{(I)}$ can for $(I) \geq 1$ be determined by:

$$c^{(I)} = \alpha^{(I)} \frac{g^{max}(\boldsymbol{x}^{(I-1)})}{g^{\text{PN}}(\boldsymbol{x}^{(I-1)})} + \left(1 - \alpha^{(I)}\right) c^{(I-1)} \tag{2.51}$$

Here g^{max} is the highest value of all constraint functions. The parameter α determines how much history to include. In the first iteration set $\alpha^{(I=1)} = 1$, and for subsequent iterations:

$$\alpha^{(I)} = \begin{cases}]0;1], & \text{if oscillating} \\ 1, & \text{otherwise} \end{cases} \tag{2.52}$$

The adaptive constraint scaling parameter is design dependent but non-differentiable. Therefore, the design sensitivity of this parameter is not included in the design sensitivity analysis. However, near optimum the scaling parameter will go towards a constant value, which means that the influence of the parameter on the sensitivities becomes less during the optimization. For a thorough review of density-based stress constrained topology optimization, see Verbart (2015).

2.2.3 Fatigue-based topology optimization

High-cycle fatigue-based topology optimization is a natural extension of stress constrained topology optimization. It is an emerging field of research, where most of the work reformulates the fatigue constraint into some sort of stress constraint. Often, the fatigue constrained topology is formulated by some damage equivalent loads where the fatigue analysis is assumed independent of design, as described in Section 2.1.3.

In Sherif et al. (2010) a DEL is established and used as basis for the topology optimization. Similarly, in Holmberg (2013); Holmberg et al. (2014); Holmberg (2016) a finite-life fatigue analysis independent of design is performed to determine equivalent fatigue stress constraints. Thus, they solve minimization of mass with both principal stress fatigue constraints and von Mises stress constraints. They use classical density-based topology optimization, and include regularization by density filtering and aggregation by P-norm functions.

In Jeong et al. (2015) topology optimization for fatigue, using the modified Goodman, the Soderberg, and the Gerber criteria is presented. The study is limited to constant and proportional loading conditions. In Lee et al. (2015) topology optimization with fatigue evaluated in frequency domain for proportional loading conditions is performed. In Svärd (2015), a method of using the weakest link theory in a topology setting is shown. The weakest link method is used to predict the probability of survival in each element. In Collet et al. (2017) a fatigue resistant design is achieved using density-based topology optimization. By using the modified Goodman relation and the Sines damage criterion, minimization of mass optimization with infinite-life fatigue constraints is demonstrated.

Topology optimization for fatigue has also been performed using gradient-free methods. In Mrzyglód (2010), commercial finite element software and a zero-order method is combined to optimize 2D structures subject to different high-cycle and low-cycle fatigue criteria.

Topology optimization for finite-life fatigue

In Paper C, we propose a method to include the entire fatigue analysis directly in the optimization formulation. Typically, Palmgren-Miner's rule is avoided because every stress cycle, in theory, constitutes a constraint. However, the cumulative nature of Palmgren-Miner's rule reduces the response from variable amplitude loading to a single number, i.e. the damage. Because of this accumulation, it is possible to formulate an adjoint design sensitivity analysis where only one adjoint equation needs to be solved per load case. Thus, the finite-life topology optimization can include large variable amplitude time-history loads with computational costs comparable to computational costs of static stress optimization. The method makes use of classical density-based optimization, the modified SIMP stiffness interpolation, and the qp-interpolation for stresses. In its current form, the method has the following requirements:

- Linear elastic material behaviour
- Quasi-static finite element analysis
- Proportional loading conditions
- Equivalent stress-based fatigue criterion

To a large extent, the method follows the fatigue modeling described in Section 2.1.3. However, due to the proportional loading condition, it is possible to perform rainflow counting directly on the loading. This is highly beneficial, as performing rainflow counting in every element can become computationally expensive.

For a given proportional load case, a reference static load $\hat{\boldsymbol{P}}$ is applied, and the reference displacements $\hat{\boldsymbol{u}}$ and reference stresses $\hat{\boldsymbol{\sigma}}$ are determined. From applying rainflow counting to the load time-series, scaling factors are obtained for both amplitudes, c_{a_i} and for mean, c_{m_i} for every load cycle i. Then, the displacement and stress amplitudes and means can be determined for every cycle i and every element e by:

$$\boldsymbol{\sigma}_{e_{a,i}} = c_{a_i}\hat{\boldsymbol{\sigma}}_e, \qquad \boldsymbol{\sigma}_{e_{m,i}} = c_{m_i}\hat{\boldsymbol{\sigma}}_e, \tag{2.53}$$

$$\boldsymbol{u}_{e_{a,i}} = c_{a_i}\hat{\boldsymbol{u}}_e, \qquad \boldsymbol{u}_{e_{m,i}} = c_{m_i}\hat{\boldsymbol{u}}_e, \tag{2.54}$$

Here $\hat{\boldsymbol{\sigma}}_e$ and $\hat{\boldsymbol{u}}_e$ are the vectors of element stresses and displacements, respectively, caused by the reference load vector $\hat{\boldsymbol{P}}$.

In order to apply a cumulative law, the stress-components must be related to an S-N curve. This can be done using an equivalent stress-based fatigue criteria, here demonstrated using the well-known Sines multiaxial fatigue criterion for proportional loading of metals (Sines, 1959). It combines contributions from all stress-components, and takes into account both mean and amplitude stresses indicated by subscripts m and a, respectively. For plane stress conditions and finite-life, the criterion in 2D can be written as (Stephens et al., 2000):

$$\sqrt{2}\tilde{\sigma}_{e_i} = \sqrt{(\sigma_{e_{ax,i}} - \sigma_{e_{ay,i}})^2 + \sigma^2_{e_{ax,i}} + \sigma^2_{e_{ay,i}} + 6\tau^2_{e_{a,i}}} + \beta\left(\sigma_{e_{mx,i}} + \sigma_{e_{my,i}}\right) \tag{2.55}$$

Here β is a material constant. $\tilde{\sigma}_{e_i}$ is an equivalent uniaxial stress state, that can be used in combination with S-N curves to find an estimated amount of cycles to failure. This can, in turn, be used with Palmgren-Miner's linear damage hypothesis to determine an accumulated damage. This is done in a similar manner as with the jacket optimization. Thus, the accumulated damage in a single load case setting is (similar to (2.22) in the jacket optimization framework):

$$D_e = c_D \sum_{i=1}^{n_i} \frac{n_i}{N_{e_i}} \leq \eta \tag{2.56}$$

c_D is a scaling constant to make the load series representative for a lifetime, and n_i is the number of cycles. The constraint must be satisfied in every element e, thus, this is computationally not viable. A P-norm function can be applied to reduce the many local constraints into one global:

$$g = \left(\sum_{e=1}^{n_e} (D_e)^P\right)^{\frac{1}{P}} \leq \eta \tag{2.57}$$

In e.g. París et al. (2010); Holmberg et al. (2013) it is suggested to use several aggregation functions distributed into regions using different approaches. However, in the authors experience, a global approach works better for the examples considered.

DSA - Finite-life fatigue

The design sensitivity analysis is performed using the adjoint method. In the constraint function (2.57), Lagrange multipliers $\boldsymbol{\lambda}$ corresponding to the amplitude and mean stress states are introduced. The augmented constraint equation $\breve{g}$ is:

$$\breve{g} = g - \sum_{i=1}^{n_i} \left(\boldsymbol{\lambda}^T_{a_i}(\boldsymbol{K}\boldsymbol{u}_{a_i} - \boldsymbol{P}_{a_i}) + \boldsymbol{\lambda}^T_{m_i}(\boldsymbol{K}\boldsymbol{u}_{m_i} - \boldsymbol{P}_{m_i})\right) \tag{2.58}$$

$\boldsymbol{u}_{a_i}$ and $\boldsymbol{u}_{m_i}$ are the vectors of amplitude displacements and mean displacements for stress cycle i, respectively. Likewise, $\boldsymbol{P}_{a_i}$ and $\boldsymbol{P}_{m_i}$ are the amplitude and mean load vectors. The above equation is, when equilibrium is satisfied, equal to the original constraint equation. Immediately, it looks as if an adjoint equation must be solved for each equilibrium state for both amplitude and mean. However, it turns out that the design sensitivity of the above equation can be determined very efficiently when exploiting the linear analysis and cumulative nature of Palmgren-Miner's rule.

We introduce a vector of the sum of scaled Lagrange multipliers, $\boldsymbol{\Lambda}$:

$$\boldsymbol{\Lambda} = \sum_{i=1}^{n_i} \left(c_{a_i} \boldsymbol{\lambda}_{a_i} + c_{m_i} \boldsymbol{\lambda}_{m_i} \right) \tag{2.59}$$

The sum of scaled Lagrange multipliers can be determined by the following adjoint equation:

$$\boldsymbol{K}\boldsymbol{\Lambda} = \sum_{i=1}^{n_i} \left(c_{a_i} \frac{\partial g^T}{\partial \boldsymbol{u}_{a_i}} + c_{m_i} \frac{\partial g^T}{\partial \boldsymbol{u}_{m_i}} \right) \tag{2.60}$$

Thus, the amount of adjoint equations is equal to the amount of load cases, and not dependent on the size of the load case (amount of cyclic loads).

By differentiating the augmented constraint function defined in (2.58) with respect to a design variable x_e, and assuming design independent loads, the design sensitivity is obtained:

$$\frac{d\breve{g}}{dx_e} = \frac{\partial g}{\partial x_e} - \boldsymbol{\Lambda}^T \frac{d\boldsymbol{K}}{dx_e} \hat{\boldsymbol{u}} \tag{2.61}$$

While several partial derivatives must be calculated for each load cycle i, they are in general computationally inexpensive. Consequently, the proposed method is very effective with computational costs comparable to static stress optimization.

The approach is described in more detail in Paper C, where examples of fatigue constrained topology optimization are given. The examples clearly demonstrate the effectiveness of the method. Moreover, they demonstrate that designs by fatigue-based topology optimization can differ from designs by stress-based topology optimization for even single load case problems.

Chapter 3

Summary of Results and Conclusion

This chapter serves as a brief summary of the included papers. Each paper will be introduced separately and the objectives, the methods, and the results of the research will be highlighted. Then, a statement of the contributions and of the impact of the work will be presented. Lastly, suggestions and recommendations for future work within this field of research are given.

3.1 Description of Papers

The following contains summaries of the included papers. The papers constitute the main contribution of this thesis.

3.1.1 Paper A

In Oest et al. (2017b) an effective method for gradient-based structural optimization of jacket structures for large offshore wind turbines is established. The optimization takes outset in a conceptual jacket design where the topology is already determined. Then, the optimization alters the cross-sectional areas of the tubular members until an optimum is found.

It is important to be able to include site- and turbine specific data in the optimization. This is considered through the loading conditions, where wave forces are calculated using the Morison equation and site-specific data. The aerodynamic loads are determined using multibody simulation software HAWC2 (Horizontal Axis Wind turbine simulation Code 2nd generation). The specific jacket investigated is the OC4 reference jacket with the NREL 5 MW reference wind turbine installed at the K13 deep water site in the North Sea off the coast of the Netherlands.

In the design of a jacket structure, extremely large load series are used to ensure that both the fatigue limit states and the ultimate limit states are satisfied. However, to reduce the computational costs of the optimization to a reasonable level, the amount of load series must be reduced. This computational cost-benefit consideration is difficult and most likely case-specific. Consequently, it is a driving goal for the proposed method to include many load series in the fatigue analysis with minimal additional computational costs. This is achieved through utilizing a quasi-static modeling approach instead of the more commonly used transient analysis.

Following common practice in industry, a Timoshenko beam finite element program is created to analyze the structure. The analysis covers most of the important structural criteria, i.e. fatigue in welded connections, overall natural frequencies, local buckling, global buckling, and shear punching and chord face failure of welded connections. These criteria are based on international design standards and recommendations. The design sensitivity analysis is performed analytically, where an adjoint approach is applied to the fatigue constraints in such a way, that the amount of adjoint equations that must be solved is independent of the amount of applied loads. Thus, a large amount of load time-histories is applied in the structural optimization where a reduction in mass of 40% as compared with the initial design is achieved. At the optimum, both fatigue and ultimate limit state constraints are active, and the active constraints are located from top to bottom of the structure.

The efficient sensitivity analysis can be applied to many multiaxial and non-proportional loaded structures, where the fatigue analysis is done in a *single number* stress-based approach. By single number, it should be understood that only one stress component (or an equivalent stress as e.g. von Mises stress) is affecting the damage. This is important such that traditional rainflow counting can be applied. For multiaxial and non-proportional loading conditions with a multiaxial fatigue criterion, more complex and computational demanding methods should be applied which is beyond the scope of this work, as fatigue damage estimation of jacket structures is solely based on the amplitude of the normal stresses.

3.1.2 Paper B

In Oest et al. (2017a) a critical evaluation of three different state-of-the-art gradient-based optimization approaches for sizing of offshore jacket structures is made. The three methods are based on (i) a static (damage equivalent load) analysis, (ii) a quasi-static analysis, and (iii) a dynamic analysis. All three optimization approaches are applied to the same optimization problem, i.e. the OC4 jacket with the NREL 5 MW baseline turbine. The optimized designs are evaluated in commercial software FEDEM Windpower. In FEDEM Windpower the jacket structures are analyzed using a transient analysis with aero-elastic simulation under inflow turbulence environment and hydrodynamic loads. Thus, the article aims to partly fill a gap in many research papers by actually evaluating the optimized design in software designed for that specific purpose. Additionally, the article aims to provide useful observations on how accurate the modeling needs to be, in an optimization setting, in order to achieve a preliminary jacket design with low mass and fatigue damage levels near the allowable level.

Using Component Object Model Application Programming Interface (COM-API), the initial and optimized jackets from the MATLAB-based DTU in-house optimization software JADOP (Jacket Design OPtimization), are exported to FEDEM Windpower using python scripts. The nodal displacements are exported back to JADOP, such that stress concentration factors can be included in the fatigue analysis. The fatigue analysis based on the multibody simulation is seen as the basis of comparison.

The initial design is evaluated for all three methods, and the dynamic analysis in JADOP showed very good agreement with the multibody analysis in FEDEM Windpower. However, the quasi-static and especially the static analysis showed inaccurate results. The static DEL approach greatly overpredicts the damage at a few hot spots, but generally underestimates the damage. The quasi-static approach also underestimates the damage. In general, the inaccuracies are due to local out-of-plane vibrations of X-connections at a structural eigenfrequency. Excitation of structural eigenfrequencies cannot be captured using quasi-static modeling.

The results showed that including a safety factor corresponding to the mean error of the analysis, acceptable designs can be achieved using all three approaches. However, the dynamic approach yields the most accurate designs. Interestingly, the fatigue damage caused by the loading conditions does not change significantly even though the designs are reduced by about half of the overall mass. Additionally, it is observed that hydrodynamic loading does not contribute significantly to the overall damage, and can thus be left out during the preliminary design phase. Load direction can have a large influence on the damage, and therefore different load directions should always be considered in the design optimization.

All designs reduce the stress concentration factors which can, in general, be achieved by reducing the diameter to thickness relation of the chords. Since this is partially design driving, the optimized designs resemble each other to a certain extent.

In conclusion, the damage equivalent load and quasi-static methods can be applied, but should only be done so with care and insight into the accuracies (or inaccuracies) in the analyses. Gradient-based optimization with a dynamic analysis is a viable and good approach to preliminary design of jacket structures.

3.1.3 Paper C

In Oest and Lund (2017) an effective method to perform fatigue-based topology optimization for variable amplitude high-cycle fatigue is developed. The method is a natural extension of conventional stress-based topology optimization. The effectiveness of the method is due to an analytical design sensitivity analysis formulation, where the computational effort is not affected much by the size of the applied load series. This is true since only one adjoint vector per load case per constraint equation must be solved. This is equivalent to e.g. static stress topology optimization.

The physics are modeled using linear finite element theory with bilinear rectangular elements. The method requires a linear analysis, thus the material is assumed linear elastic and the analysis is quasi-static. While a linear quasi-static method can be a crude estimation, it is very effective for high-cycle fatigue as the structural response can be found very effectively. In this framework, the structural response is determined for reference loads. Then, the response for the reference load with different load magnitudes can be found using linear superposition. To avoid the so-called checkerboard patterns, consistent density filtering is applied.

The fatigue analysis is included directly in the optimization and is performed using a standard approach. The damage is estimated using the multiaxial Sines method. The Sines method is an equivalent-stress method that includes contributions from all stress amplitude components as well as the mean normal stresses. The Sines method is limited to proportional loading conditions. Due to the restriction of proportional loading, amplitude and mean load scaling factors can be found by performing standard rainflow counting on the load spectrum. Thus, amplitude and mean stresses and displacements can be determined efficiently. The cumulative damage is determined using Palmgren-Miner's linear damage hypothesis.

The stress components, and thus the accumulated fatigue, are evaluated at the superconvergent center point in each finite element. Consequently, the number of constraints is equal to the number of design variables. To maintain computational efficiency, the local constraints are aggregated into a global constraint using the P-norm method. The P-norm approximates the largest local constraint, and in this framework, the accuracy is improved using adaptive constraint scaling.

To address the singular optima that can arise in stress and fatigue optimization with vanishing constraints, stress relaxation using the qp-method is applied. This method expands the design space and penalize stresses for intermediate densities effectively.

Since Palmgren-Miner's method is used, an adjoint formulation can be applied where the sum of Lagrange multipliers are solved in the adjoint problem. This makes the method very effective for even large load series.

Three examples are studied, where the first example is a clamped L-plate. This example is with fully reversed loading conditions, which will give a fatigue optimized design that is intuitively easy to understand and that resembles a stress optimized design. Additionally, two more examples are presented where the loading condition is not fully reversed. Thus, the mean effects will affect the design such that it no longer resembles a stress optimized design. These examples clearly demonstrate the effectiveness of the method, and why it can be very beneficial to use fatigue constrained topology optimization.

3.2 Conclusions and contributions

The overall aim of this work is to develop efficient methods for structural optimization with fatigue constraints. The proposed methods are generic and stand as novel contributions to fatigue-based structural optimization. The main contributions from each paper are:

- In Paper A, an extensive framework of jacket optimization was established including many constraints based on standards, and large load series. The main outcome is a generic method for structural optimization with fatigue constraints under multiaxial and non-proportional loading conditions. In the approach, fatigue contributions were limited to normal stresses according to standards, but this can easily be altered to a fatigue analysis based on equivalent stress-based methods. The approach scales well with large load series. Due to quasi-static modeling, direct computation of the fatigue gradients is possible. Thus, memory problems is not an issue for even very large load series.

- In Paper B, a gap in optimization of substructures for wind turbines is addressed, i.e. critical post-processing of the optimized structure. By applying three different methods to structural optimization of a jacket structure within a single framework, a fair comparison is made. It is observed that damage caused by aerodynamic loading does not change significantly for large sizing changes of the substructure. This finding is key to the success of current frameworks on gradient-based optimization of jacket structures.
- In Paper C, a generic method for topology optimization of continua with fatigue constraints is presented. Contrary to most efforts in the field, the entire fatigue analysis is included in the optimization formulation. By doing so, the cumulative nature of Palmgren-Miner's rule can be exploited. In combination with an aggregation function, it reduces the problem to a single overall constraint, where only a single adjoint equation must be solved for each load case. Additionally, the method is directly applicable to 3D problems.

3.3 Future work

The presented research can be extended in many ways. The work in Paper A demonstrated that a large amount of criteria and load cases can be included in a jacket optimization framework. Adding options for including the transition piece and the turbine tower in the optimization framework will make it an even more powerful design tool. Because jackets are very stiff structures, it can be difficult to adjust the structural frequencies to be within the desired frequency bands. Including both tower and transition piece will help address this issue.

Very limited work has been done with topology optimization of jacket structures. However, with an effective topology optimization with beam elements performed prior to a sizing optimization, the preliminary design phase will be even more efficient, and less knowledge about the initial design is required. Parameterizing the jacket into different modules, e.g. based on entire sections, can be a viable approach for large offshore wind farms which allows for mass production. This optimization problem can be solved by e.g. integer programming or the Discrete Material Optimization (DMO) approach (Stegmann and Lund, 2005).

Although comprehensive, the study in Paper B is still very limited. Naturally, the study can be extended to other jackets and wind turbines, and to investigate the influence of soil-structure interaction, wind speeds, buoyancy, etc. Also, more insight into how the aerodynamic loading and aerodynamic damping changes with alterations in the substructure can be important. This is coupled with another important prospect, i.e. identification and correction methods to make computational efficient methods such as the damage equivalent load more applicable. If a method is developed such that the accuracy of damage equivalent loads is guaranteed within an acceptable level, gradient-based optimization of jacket structures for preliminary designs can be performed with limited computational effort.

In Paper C, the topology optimization method can, and should, be extended to 3D structures with an equivalent stress-based fatigue criteria. However, to improve the method significantly, the method must be applicable to 3D problems with multiaxial and non-proportional loading conditions. Typically, this means that critical plane methods (see e.g. Socie and Marquis (1999); Karolczuk and Macha (2005)) should be applied. Using critical plane methods and 3D solid elements, even the analysis itself becomes computationally expensive. Rainflow counting must be performed separately in each element, and the critical plane must be determined individually for each element. Additionally, the sensitivity of the critical plane must be determined in an efficient manner. Combined with the high computational costs and the very non-linear behaviour of fatigue, this is a challenging task. It is the authors recommendation that 3D topology optimization with multiaxial and non-proportional fatigue-loading should only be pursued by using performance oriented coding language with parallel computing.

If an effective method for 3D topology optimization with fatigue constraints is established, a great industrial application would be the optimization of a transition piece for a wind turbine support structure. It involves complicated boundaries and large load series, but is still typically modeled with linear elastic material (steel) and with a linear finite element analysis. Additionally, industry has not settled on a single transition piece design that is considered the best.

References

JS Arora, AI Chahande, and JK Paeng. Multiplier methods for engineering optimization. *International Journal for Numerical Methods in Engineering*, 32(7):1485–1525, 1991.

T Ashuri, MB Zaaijer, JRRA Martins, GJW van Bussel, and GAM van Kuik. Multidisciplinary design optimization of offshore wind turbines for minimum levelized cost of energy. *Renewable Energy*, 68:893–905, 2014.

T Ashuri, C Ponnurangam, J Zhang, and M Rotea. Integrated Layout and Support Structure Optimization for Offshore Wind Farm Design. In *Journal of Physics: Conference Series*, volume 753, page 92011, 2016.

MP Bendsøe. Optimal shape design as a material distribution problem. *Structural optimization*, 1(4):193–202, 1989.

MP Bendsøe and O Sigmund. Material interpolation schemes in topology optimization. *Archive of Applied Mechanics*, 69(9):635–654, 1999.

MP Bendsøe and O Sigmund. *Topology Optimization - Theory, Methods, and Applications*. Springer-Verlag Berlin Heidelberg, 2 edition, 2004.

B Bourdin. Filters in topology optimization. *International Journal for Numerical Methods in Engineering*, 50(9):2143–2158, 2001.

M Bruggi. On an alternative approach to stress constraints relaxation in topology optimization. *Structural and Multidisciplinary Optimization*, 36(2):125–141, 2008.

M Bruggi and P Duysinx. Topology optimization for minimum weight with compliance and stress constraints. *Structural and Multidisciplinary Optimization*, 46(3): 369–384, 2012.

M Bruggi and P Duysinx. A stress–based approach to the optimal design of structures with unilateral behavior of material or supports. *Structural and Multidisciplinary Optimization*, 48(2):311–326, 2013.

M Bruggi and P Venini. A mixed FEM approach to stress-constrained topology optimization. *International Journal for Numerical Methods in Engineering*, 73(12):1693–1714, 2008.

TE Bruns and DA Tortorelli. Topology optimization of non-linear elastic structures and compliant mechanisms. *Computer Methods in Applied Mechanics and Engineering*, 190(26):3443–3459, 2001.

GD Cheng and X Guo. ϵ-relaxed approach in structural topology optimization. *Structural optimization*, 13(4):258–266, 1997.

K-H Chew. *Optimal structural design for offshore wind energy system*. Phd thesis, Nanyan Technological University, 2017.

K-H Chew, M Muskulus, S Narasimalu, K Tai, and EYK Ng. Fatigue sensitivity analysis of offshore wind turbine structures. *Proceedings of WCSMO-11*, pages 798–803, 2015.

K-H Chew, K Tai, EYK Ng, and M Muskulus. Analytical gradient-based optimization of offshore wind turbine substructures under fatigue and extreme loads. *Marine Structures*, 47:23–41, 2016.

RW Clough and J Penzien. *Dynamics of Structures*. McGraw-Hill, 1975.

M Collet, M Bruggi, and P Duysinx. Topology optimization for minimum weight with compliance and simplified nominal stress constraints for fatigue resistance. *Structural and Multidisciplinary Optimization*, 55(3):839–855, 2017.

RD Cook, DS Malkus, ME Plesha, and RJ Witt. *Concepts and applications of finite element analysis*. John Wiley & Sons, New York, N.Y., 4th ed. edition, 2002.

GA da Silva, AT Beck, and EL Cardoso. Topology optimization of continuum structures with stress constraints and uncertainties in loading. *International Journal for Numerical Methods in Engineering*, pages 1–33, 2017.

W de Vries. Support structure concepts for deep water sites. Technical report, Delft University of Technology, Delft, 2011.

JD Deaton and RV Grandhi. A survey of structural and multidisciplinary continuum topology optimization: post 2000. *Structural and Multidisciplinary Optimization*, 49 (1):1–38, 2014.

K Deb, A Pratap, S Agarwal, and T Meyarivan. A fast and elitist multiobjective genetic algorithm: NSGA-II. *IEEE transactions on evolutionary computation*, 6(2):182–197, 2002.

DNV. *DNV-OS-J101: Design of Offshore Wind Turbine Structures*. Det Norske Veritas, Høvik, 2013.

DNV. *RP-C203: Fatigue design of offshore steel structures*. Det Norske Veritas, Høvik, 2014.

P Duysinx and MP Bendsøe. Topology optimization of continuum structures with local stress constraints. *International Journal for Numerical Methods in Engineering*, 43 (8):1453–1478, 1998.

P Duysinx and O Sigmund. New developments in handling stress constraints in optimal material distribution. *7th AIAA/USAF/NASA/ISSMO Symposium on Multidisciplinary Analysis and Optimization*, 1998.

M Efthymiou. Development of SCF formulae and generalised influence functions for use in fatigue analysis. *Proceedings of the Offshore Tubular Joints Conference*, pages 1–13, 1988.

M Efthymiou and S Durkin. Stress concentrations in T/Y and gap/overlap K-joints. *Proceedings of the 4th International Conference on Behaviour of Offshore Structures*, pages 1–12, 1985.

A Fatemi and N Shamsaei. Multiaxial fatigue: An overview and some approximation models for life estimation. *International Journal of Fatigue*, 33(8):948–958, 2011.

T Fischer, W de Vries, and B Schmidt. UpWind Design Basis. Technical report, 2010.

G Freebury and W Musial. Determining equivalent damage loading for full-scale wind turbine blade fatigue tests. In *2000 ASME Wind Energy Symposium*, page 50, 2000.

T Gentils, L Wang, and A Kolios. Integrated structural optimisation of offshore wind turbine support structures based on finite element analysis and genetic algorithm. *Applied Energy*, 199:187–204, 2017.

N Gerzen, PM Clausen, S Suresh, and CBW Pedersen. Fatigue Sensitivities for Sizing Optimization of Shell Structures. In *Proceedings of the 12th World Congress on Structural and Multidisciplinary Optimization*, pages 1–13, Braunschweig, 2017.

K Hasselmann, TP Barnett, E Bouws, H Carlson, DE Cartwright, K Enke, JA Ewing, H Gienapp, DE Hasselmann, P Kruseman, A Meerburg, P Muller, DJ Olbers, K Richter, W Sell, and H Walden. Measurements of Wind-Wave Growth and Swell Decay during the Joint North Sea Wave Project (JONSWAP). Technical Report 8 0, 1973.

E Holmberg. *Stress and fatigue constrained topology optimization*. Licentiate thesis no. 1571, Linköping University, 2013.

E Holmberg. *Topology optimization considering stress, fatigue and load uncertainties*. Phd thesis, Linköping University, 2016.

E Holmberg, B Torstenfelt, and A Klarbring. Stress constrained topology optimization. *Structural and Multidisciplinary Optimization*, 48(1):33–47, 2013.

E Holmberg, B Torstenfelt, and A Klarbring. Fatigue constrained topology optimization. *Structural and Multidisciplinary Optimization*, 50(2):207–219, 2014.

IEC. *IEC 61400-1 Wind Turbines - Part 1: Design requirements*, volume 2005. International Electrotechnical Commission, Geneva, 2005.

IEC. *IEC 61400-3 Wind Turbines - Part 3: Design requirements for offshore wind turbines*. International Electrotechnical Commission, Geneva, 2009.

International Renewable Energy Agency. Renewable Power Generation Costs in 2014. Technical report, 2015.

MZ Jacobson and CL Archer. Saturation wind power potential and its implications for wind energy. *Proceedings of the National Academy of Sciences*, 109(39):15679–15684, 2012.

SH Jeong, SH Park, D-H Choi, and GH Yoon. Topology optimization considering static failure theories for ductile and brittle materials. *Computers & Structures*, 110: 116–132, 2012.

SH Jeong, D-H Choi, and GH Yoon. Fatigue and static failure considerations using a topology optimization method. *Applied Mathematical Modelling*, 39(3):1137–1162, 2015.

J Jonkman, S Butterfield, W Musial, and G Scott. Definition of a 5-MW reference wind turbine for offshore system development. Technical Report February, 2009.

A Karolczuk and E Macha. A Review of Critical Plane Orientations in Multiaxial Fatigue Failure Criteria of Metallic Materials. *International Journal of Fracture*, 134 (3):267, 2005.

J Kennedy. Particle swarm optimization. In *Encyclopedia of machine learning*, pages 760–766. Springer, 2011.

S Kirkpatrick, CD Gelatt, and MP Vecchi. Optimization by simulated annealing. *Science*, 220(4598):671–680, 1983.

U Kirsch. On singular topologies in optimum structural design. *Structural optimization*, 2(3):133–142, 1990.

EI Konstantinidis and PN Botsaris. Wind turbines: current status, obstacles, trends and technologies. *IOP Conference Series: Materials Science and Engineering*, 161(1): 12079, 2016.

G Kreisselmeier and R Steinhauser. Systematic Control Design By Optimizing a Vector Performance Index. In *Computer Aided Design of Control Systems*, pages 113–117. 1980.

C Le, J Norato, TE Bruns, C Ha, and DA Tortorelli. Stress-based topology optimization for continua. *Structural and Multidisciplinary Optimization*, 41(4):605–620, 2010.

E Lee, KA James, and JRRA Martins. Stress-Constrained Topology Optimization with Design-Dependent Loading. *Structural and Multidisciplinary Optimization*, 46:647–661, 2012.

JW Lee, GH Yoon, and SH Jeong. Topology optimization considering fatigue life in the frequency domain. *Computers & Mathematics with Applications*, 70(8):1852–1877, 2015.

H Lian, AN Christiansen, DA Tortorelli, O Sigmund, and N Aage. Combined shape and topology optimization for minimization of maximal von Mises stress. *Structural and Multidisciplinary Optimization*, 55(5):1541–1557, 2017.

H Long and G Moe. Preliminary design of bottom-fixed lattice offshore wind turbine towers in the fatigue limit state by the frequency domain method. *Journal of Offshore Mechanics and Arctic Engineering*, 134(3):31902–10, 2012.

H Long, G Moe, and T Fischer. Lattice towers for bottom-fixed offshore wind turbines in the ultimate limit state: variation of some geometric parameters. *Journal of Offshore Mechanics and Arctic Engineering*, 134(2):021202–13, 2011.

Y Luo and Z Kang. Topology optimization of continuum structures with Drucker–Prager yield stress constraints. *Computers & Structures*, 90:65–75, 2012.

Y Luo, MY Wang, and Z Deng. Stress-based topology optimization of concrete structures with prestressing reinforcements. *Engineering Optimization*, 45(11):1349–1364, 2013a.

Y Luo, MY Wang, and Z Kang. An enhanced aggregation method for topology optimization with local stress constraints. *Computer Methods in Applied Mechanics and Engineering*, 254:31–41, 2013b.

M Matsuishi and T Endo. Fatigue of metals subjected to varying stress. *Japan Society of Mechanical Engineering*, 68(2):37–40, 1968.

MA Miner. Cumulative Damage in Fatigue. *Journal of Applied Mechanics*, 12(3):A159–A164, 1945.

JR Morison, MP O'Brien, JW Johnson, and SA Schaaf. The Force Exerted by Surface Waves on Piles. *Journal of Petroleum Technology*, 2(5):149–154, 1950.

M Mrzyglód. Multiaxial HCF and LCF Constraints in Topology Optimization. In *The Ninth International Conference on Multiaxial Fatigue and Fracture*, pages 803–810, Parma, 2010.

M Muskulus and S Schafhirt. Design optimization of wind turbine support structures - a review. *Journal of Ocean and Wind Energy*, 1(1):12–22, 2014.

F Navarrina, I Muiños, I Colominas, and M Casteleiro. Topology optimization of structures: A minimum weight approach with stress constraints. *Advances in Engineering Software*, 36(9):599–606, 2005.

J Oest and E Lund. Topology optimization with finite-life fatigue constraints. *Structural and Multidisciplinary Optimization*, pages 1–15, 2017. doi: 10.1007/s00158-017-1701-9.

J Oest, K Sandal, S Schafhirt, LES Stieng, and M Muskulus. On analytical gradient-based optimization of jacket structures for offshore wind turbines. *under review*, pages 1–15, 2017a.

J Oest, R Sørensen, LCT Overgaard, and E Lund. Structural optimization with fatigue and ultimate limit constraints of jacket structures for large offshore wind turbines. *Structural and Multidisciplinary Optimization*, 55(3):779–793, 2017b.

AG Palmgren. Die Lebensdauer von Kugellagern. *Zeitschrift des Vereines Deutscher Ingenieure*, 14:339–341, 1924.

J París, F Navarrina, I Colominas, and M Casteleiro. Topology optimization of continuum structures with local and global stress constraints. *Structural and Multidisciplinary Optimization*, 39(4):419–437, 2009.

J París, F Navarrina, I Colominas, and M Casteleiro. Block aggregation of stress constraints in topology optimization of structures. *Advances in Engineering Software*, 41(3):433–441, 2010.

LB Pasamontes, FG Torres, D Zwick, S Schafhirt, and M Muskulus. Support structure optimization for offshore wind turbines with a genetic algorithm. In *Proceedings of the ASME 2014 33rd Internation Conference on Ocean, Offshore and Arctic Engineering*, pages 1–7, San Fransisco, 2014.

P Passon and K Branner. Load calculation methods for offshore wind turbine foundations. *Ships and Offshore Structures*, 9(4):433–449, 2013.

JT Pereira, EA Fancello, and CS Barcellos. Topology optimization of continuum structures with material failure constraints. *Structural and Multidisciplinary Optimization*, 26(1):50–66, 2004.

A Perelmuter and V Yurchenko. Parametric Optimization of Steel Shell Towers of High-Power Wind Turbines. *Procedia Engineering*, 57:895–905, 2013.

S Qyatt, A-K Govindji, R James, N Duan, B Xie, M Liu, and G Yi. Detailed appraisal of the offshore wind industry in China. Technical report, The Carbon Trust, 2014.

RP Reed, JH Smith, and BW Christ. The Economic Effects of Fracture in the United States. Technical report, U.S Department of Commerce, National Bureau of Standards, 1983.

GIN Rozvany. A critical review of established methods of structural topology optimization. *Structural and Multidisciplinary Optimization*, 37(3):217–237, 2009.

S Schafhirt, D Zwick, and M Muskulus. Reanalysis of Jacket Support Structure for Computer-Aided Optimization of Offshore Wind Turbines with a Genetic Algorithm. In *Proceedings of the Twenty-fourth International Ocean and Polar Engineering Conference*, pages 234–241, Busan, 2014.

S Schafhirt, D Zwick, and M Muskulus. Two-stage local optimization of lattice type support structures for offshore wind turbines. *Ocean Engineering*, 117:163–173, 2016.

M Seidel. Substructures for offshore wind turbines - Current trends and developments. *Festschrift Peter Schaumann*, pages 1–6, 2014.

K Sherif, W Witteveen, K Puchner, and H Irschik. Efficient Topology Optimization of Large Dynamic Finite Element Systems Using Fatigue. *AIAA Journal*, 48(8):1339–1347, 2010.

O Sigmund. Morphology-based black and white filters for topology optimization. *Structural and Multidisciplinary Optimization*, 33(4):401–424, 2007.

O Sigmund and K Maute. Topology optimization approaches. *Structural and Multidisciplinary Optimization*, 48(6):1031–1055, 2013.

O Sigmund and J Petersson. Numerical instabilities in topology optimization: A survey on procedures dealing with checkerboards, mesh-dependencies and local minima. *Structural optimization*, 16(1):68–75, 1998.

G Sines. Behavior of Metals Under Complex Static and Alternating Stresses. *Metal Fatigue*, pages 145–169, 1959.

D Socie and G Marquis. Multiaxial fatigue. *Society of Automotive Engineers, 1999. 502*, pages 1–484, 1999.

J Stegmann and E Lund. Discrete material optimization of general composite shell structures. *International Journal for Numerical Methods in Engineering*, 62(14):2009–2027, 2005.

RI Stephens, A Fatemi, RR Stephens, and HO Fuchs. *Metal Fatigue in Engineering*. A Wiley-Interscience publication. John Wiley & Sons, 2 edition, 2000.

M Stolpe and K Svanberg. An alternative interpolation scheme for minimum compliance topology optimization. *Structural and Multidisciplinary Optimization*, 22(2): 116–124, 2001a.

M Stolpe and K Svanberg. On the trajectories of the epsilon-relaxation approach for stress-constrained truss topology optimization. *Structural and Multidisciplinary Optimization*, 21(2):140–151, 2001b.

H Svärd. *Topology Optimization of Fatigue-Constrained Structures*. PhD thesis, KTH Royal Institute of Technology, 2015.

G Sved and Z Ginos. Structural optimization under multiple loading. *International Journal of Mechanical Sciences*, 10(10):803–805, 1968.

The Carbon Trust. Detailed appraisal of offshore wind industry in China. Technical report, 2014.

A Thiry, L Bair, GR Buldgen, and P Rigo. Optimization of monopile offshore wind structures. In *Proceedings of the 3rd international conference on marine structures*, pages 633–642, 2011.

DA Tortorelli and P Michaleris. Design sensitivity analysis: Overview and review. *Inverse Problems in Science and Engineering*, 1(1):71–105, 1994.

PE Uys, J Farkas, K Jármai, and F van Tonder. Optimisation of a steel tower for a wind turbine structure. *Engineering Structures*, 29(7):1337–1342, 2007.

B Valpy and P English. Future renewable energy costs: offshore wind. Technical report, BVG Associates, Eindhoven, 2014.

A Verbart. *Topology Optimization with Stress Constraints*. Phd thesis, TU Delft, 2015.

F Vorpahl, D Kaufer, and W Popko. Description of a basic model of the "Upwind reference jacket" for code camparison in the OC4 project under IEA Wind Annex 30". Technical report, Institute for Wind Energy and Energy Systems Technology, 2011.

S Wang, E de Sturler, and GH Paulino. Large-scale topology optimization using preconditioned Krylov subspace methods with recycling. *International Journal for Numerical Methods in Engineering*, 69(12):2441–2468, 2007.

JD Wheeler. Method for calculating forces produced by irregular waves. *Journal of Petroleum Technology*, pages 359–367, 1970.

RJ Yang and CJ Chen. Stress-based topology optimization. *Structural optimization*, 12 (2):98–105, 1996.

S Yoshida. Wind Turbine Tower Optimization Method Using a Genetic Algorithm. *Wind Engineering*, 30(6):453–470, 2006.

D Zwick, M Muskulus, and G Moe. Iterative optimization approach for the design of full-height lattice towers for offshore wind turbines. *Energy Procedia*, 24(0):297–304, 2012.

Paper A

Structural optimization with fatigue and ultimate limit constraints of jacket structures for large offshore wind turbines

Jacob Oest, René Sørensen, Lars Chr. T. Overgaard, Erik Lund

The paper has been published in
Structural and Multidisciplinary Optimization Vol. 55(3), pp. 779–793, 2017.
doi:10.1007/s00158-016-1527-x

Click here for access to paper

Paper B

On gradient-based optimization of jacket structures for offshore wind turbines

Jacob Oest, Kasper Sandal, Sebastian Schafhirt, Lars Einar S. Stieng, Michael Muskulus

The paper is under review

Paper C

Topology optimization with finite-life fatigue constraints

Jacob Oest, Erik Lund

The paper has been published in
Structural and Multidisciplinary Optimization, online first, pp. 1–15, 2017.
doi:10.1007/s00158-017-1701-9

Click here for access to paper

ISSN (online): 2446-1636
ISBN (online): 978-87-7210-034-0

AALBORG **UNIVERSITY PRESS**